INFLUENCE OF SURFACE TREATMENT AND HUMIDITY ON STRENGTH OF E-GLASS FIBER BUNDLES

BY

AMANDA KAY DAVIS

B.S., University of Illinois, 1997

THESIS

Submitted in partial fulfillment of the requirements
for the degree of Master of Science in Theoretical and Applied Mechanics
in the Graduate College of the
University of Illinois at Urbana-Champaign, 1999

Urbana, Illinois

This thesis is dedicated to the memory
of my grandmother, A. Geraldine King

Acknowledgments

I would like to acknowledge the financial support provided by Owens-Corning, Inc. (under the guidance of Doug Lyle). I would like to thank my advisor, Prof. Nancy R. Sottos, for her guidance, support, and patience throughout my undergraduate and graduate studies. Without her, I may have never pursued a graduate degree. I would like to thank Prof. James W. Phillips for his dedication throughout my studies in TAM. I would also like to thank the TAM machine shop for cutting so many end tabs, and Dr. Peter Kurath of AMTEL for the use of the Instron. Additionally, I would like to acknowledge the work of the undergraduates who helped with specimen production. Finally, I would like to thank my parents and friends for their love and support.

Table of Contents

Chapter Page

List of Tables..... vii

List of Figures..... ix

1 Introduction..... 1
- 1.1 Glass fiber reinforcement..... 1
- 1.2 Glass fiber manufacture and surface treatments..... 2
- 1.3 Strength of individual glass fibers..... 3
  - 1.3.1 Background..... 3
  - 1.3.2 Statistical models of failure..... 3
- 1.4 Strength of glass fiber bundles..... 6
  - 1.4.1 Statistical models..... 6
  - 1.4.2 Influences on glass fiber bundle strength..... 8
- 1.5 Overview of thesis..... 9

2 Experimental Procedure..... 13
- 2.1 Overview..... 13
- 2.2 Test matrix..... 13
- 2.3 Sample preparations..... 14
- 2.4 Environmental conditioning..... 15
- 2.5 Experimental apparatus..... 16
- 2.6 Data reduction..... 17

3 Effects of Humidity Aging..... 29
- 3.1 Overview..... 29
- 3.2 Starch surface treatment..... 29
- 3.3 Silane and starch surface treatment..... 30
- 3.4 Wax and starch surface treatment..... 30
- 3.5 Epoxy surface treatment..... 31
- 3.6 Comparison of surface treatments..... 32
- 3.7 Fiber diameter measurements..... 35
- 3.8 Acoustic emission waveforms..... 36
- 3.9 Reversibility of moisture effects..... 36
- 3.10 Effect of oven drying..... 37

4 Effects of Twist..... 59
- 4.1 Introduction..... 59
- 4.2 Experimental results..... 61

5 Conclusions..... 68
- 5.1 Future work..... 70

Appendix.....…….....…72

List of References.....….85

Vita.....….87

List of Tables

Table 1.1. Composition of E-glass used for fiber manufacture in percent weight 1
Table 2.1. Summary of fiber surface treatments 14
Table 3.1. Averages and standard deviations of tensile data for each surface treatment at 10% RH 38
Table 3.2. Averages and standard deviations of tensile data for each surface treatment at 40% RH 38
Table 3.3. Averages and standard deviations of tensile data for each surface treatment at 80% RH 38
Table 3.4. Averages and standard deviations of tensile data for each surface treatment at 100% RH 38
Table 3.5. Averages and standard deviations of tensile data for moisture reversibility data 39
Table 3.6. Averages and standard deviations of tensile data for OD + 40% RH and OD + 100% RH 39
Table 3.7. Fiber diameters measured from the first breaks and remaining unbroken fibers 35
Table 4.1. Averages and standard deviations of tensile data for type I bundles conditioned at 40% RH and twisted 0, 1, 2, 3, and 5 turns/inch 61
A.1. Table of tensile data for type I bundles conditioned at 10% RH 72
A.2. Table of tensile data for type I bundles conditioned at 40% RH 73
A.3. Table of tensile data for type I bundles conditioned at 80% RH 74
A.4. Table of tensile data for type I bundles conditioned at 100% RH 74
A.5. Table of tensile data for type II bundles conditioned at 10% RH 75
A.6. Table of tensile data for type II bundles conditioned at 40% RH 75
A.7. Table of tensile data for type II bundles conditioned at 80% RH 76
A.8. Table of tensile data for type II bundles conditioned at 100% RH 76
A.9. Table of tensile data for type III bundles conditioned at 10% RH 77
A.10. Table of tensile data for type III bundles conditioned at 40% RH 77
A.11. Table of tensile data for type III bundles conditioned at 80% RH 78
A.12. Table of tensile data for type III bundles conditioned at 100% RH 78
A.13. Table of tensile data for type IV bundles conditioned at 10% RH 79
A.14. Table of tensile data for type IV bundles conditioned at 40% RH 79
A.15. Table of tensile data for type IV bundles conditioned at 80% RH 80
A.16. Table of tensile data for type IV bundles conditioned at 100% RH 80
A.17. Table of tensile data for type I bundles conditioned at 100% RH then 10% RH for 1 hour 81
A.18. Table of tensile data for type I bundles conditioned at 100% RH, then 10% RH for 24 hour 81
A.19. Table of tensile data for type I bundles conditioned at 100% RH, then 10% RH for 48 hour 81
A.20. Table of tensile data for type II bundles oven-dried, then conditioned at 40% RH 82

A.21. Table of tensile data for type II bundles oven-dried, then conditioned at 100% RH..... 82
A.22. Table of tensile data for type I bundles twisted 1 turn/inch.....83
A.23. Table of tensile data for type I bundles twisted 2 turns/inch..... 83
A.24. Table of tensile data for type I bundles twisted 3 turns/inch..... 84
A.25. Table of tensile data for type I bundles twisted 5 turns/inch..... 84

List of Figures

Fig. 1.1. Sample reaction of silane coupling agent with water..... 10
Fig. 1.2. Histogram of break strength for fibers in a bundle (Hull, 1981)..... 10
Fig. 1.3. Plot of the probability density for different values of the Weibull modulus, β..... 11
Fig. 1.4. Ratio of bundle strength to average fiber strength as a function of the Weibull modulus..... 12
Fig. 2.1. Finished glass fiber bundle tensile specimen.....19
Fig. 2.2. Silicone rubber mold.....20
Fig. 2.3. Glass fiber in mold on bench..... 21
Fig. 2.4. Humidity chamber connected to vacuum-pump and desiccant column..22
Fig. 2.5. Tension test setup.....23
Fig. 2.6. Schematic of test setup.....24
Fig. 2.7. AE sensor attached to specimen.....25
Fig. 2.8. Typical waveform recorded by oscilloscope..... 26
Fig. 2.9. Typical load–strain plot..... 27
Fig. 2.10. Typical Weibull plot..... 28
Fig. 3.1. Representative load–strain data for type I bundles at each humidity level.....40
Fig. 3.2. Representative Weibull plot for type I bundles at each humidity level.....41
Fig. 3.3. Representative load–strain data for type II bundles at each humidity level.....42
Fig. 3.4. Representative Weibull plot for type II bundles at each humidity level.....43
Fig. 3.5. Representative load–strain data for type III bundles at each humidity level.....44
Fig. 3.6. Representative Weibull plot for type III bundles at each humidity level.....45
Fig. 3.7. Representative load–strain data for type IV bundles at each humidity level.....46
Fig. 3.8. Representative Weibull plot for type IV bundles at each humidity level.....47
Fig. 3.9. Comparison of average peak load for each surface treatment at 10% and 100% RH levels.....48
Fig. 3.10. Comparison of average number of breaks at peak for each surface treatment at 10% and 100% RH... 49
Fig. 3.11. Comparison of average strain to failure for each surface treatment at 10% and 100% RH..... 50
Fig. 3.12. Comparison of the average Weibull modulus for each surface treatment at 10% and 100% RH.....51
Fig. 3.13 Typical cross-section of a glass fiber bundle……..52
Fig. 3.14. Typical waveform for type I bundles conditioned at 40% RH..... 53
Fig. 3.15. Typical waveform for type II bundles conditioned at 40% RH..... 53

Fig. 3.16. Typical waveform for type III bundles conditioned at 40% RH..... 54
Fig. 3.17. Signal recorded during tension test of type III bundle conditioned at 40% RH..... 54
Fig. 3.18. Typical waveform for type IV bundles conditioned at 40% RH..... 55
Fig. 3.19. Signal recorded during tension test of type IV bundle conditoned at 40% RH..... 55
Fig. 3.20. Representative load–strain data for type I bundles conditioned at 10% RH only and at 100% RH for 24 hours followed by 10% RH for 1, 24, and 48 hours intervals..... 56
Fig. 3.21. Comparison of average peak loads for type I bundles conditioned at 100% RH then 0, 1, 24, and 48 hours at 10% RH and 10% RH only..... 57
Fig. 3.22. Representative load–strain plot for OD + 40% and OD + 100 type II bundles..... 58
Fig. 4.1. Model for the tensile strength of twisted yarn..... 63
Fig. 4.2. Representative load–strain plot for type I at all levels of twist.....64
Fig. 4.3. Comparison of average peak load for each increase in the number of turns/inch.....65
Fig. 4.4. Comparison of number of breaks at peak load for each increase in the number of turns/inch.....66
Fig. 4.5. Comparison of the Weibull modulus for each increase in the number of turns/inch..... 67

Chapter 1

Introduction

1.1 Glass fiber reinforcement

Glass fiber reinforcement is used in a wide variety of applications, such as tapes, circuit board substrates, polymer matrix composites, and insulation. A key advantage of glass fiber reinforcement is its high strength to weight ratio. As the diameter of a fiber becomes smaller, the strength of a virgin glass fiber can exceed 3.0 GPa. However, the strength of commercial fibers is much lower due to damage from contact abrasion or environmental corrosion.

The most common type of glass used for fibers is electrical glass, or E-glass. E-glass has good strength, stiffness, electrical, and weathering properties. The composition of mineral glasses is based on silica with additions of oxides of calcium, boron, sodium, iron, and aluminum. The composition of E-glass is listed in Table 1.1 (Hull, 1991).*

Table 1.1. Composition of E-glass used for fiber manufacture in percent weight.

Chemical	Composition (%wt)
SiO_2	52.4
Al_3O_3, Fe_2O_3	14.4
CaO	17.2
MgO	4.6
Na_2O, K_2O	0.8
Ba_2O_3	10.6

* References to the literature are listed alphabetically by author, beginning on page 84.

1.2 Glass fiber manufacture and surface treatments

The manufacturing of glass fibers begins with melting the raw materials in a tank that feeds into a series of platinum bushings with several hundred holes in the base of each bushing. Gravity feeds the glass through the bushings, then fine filaments are mechanically drawn downwards as the glass flows through the holes. The fibers are quenched by a light water spray, then passed over a belt to apply a surface treatment, or size. The filaments are then gathered together into a bundle and wound onto bobbins at very high speeds. The diameter of the filaments, typically 8 to 15 μm, is controlled by the temperature of the glass, the diameter of the holes, and the winding speed (Agarwal and Broutman, 1990). The number of filaments in the bundle can range from fifty to several thousand.

A size is a thin coating applied to the fibers to protect the surface from damage, to lubricate the fibers during manufacturing, to minimize static, or to enhance interfacial bonding with a binder or matrix. For example, wax coatings lubricate during weaving, while epoxy sizes enhance interfacial ashesion. Silane surface treatments are commonly used to promote adhesion and protect against moisture damage.

Silane coupling agents are of the general chemical structure $X_3Si—R—Y$, where Y is the group that would bond to a binder or polymer matrix when the fibers are embedded and X is a hydrolyzable group. As shown schematically in Fig. 1.1,[†] the hydrolyzable group may form Si—OH bonds in water or may react with the mineral, M, of the glass to

[†] Figures are collected at the end of each chapter.

form M—OH bonds. The silane coupling agent also keeps water molecules in an equilibrium reaction outside of the glass so the water will not react with the glass fiber (Plueddemann, 1991).

1.3 Strength of individual glass fibers

1.3.1 Background

The strength of E-glass fibers is not easily characterized by a single average value. Figure 1.2 shows a sample histogram of break strengths for glass fibers (Hull 1981). Statistical models are used to describe the distribution of glass fiber strength because a distribution of strengths is found when testing many fibers. This section outlines the well-known model derived by Coleman (1958), which applies the Weibull distribution to characterize the strength of single glass filaments.

1.3.2 Statistical models of failure

Coleman assumed each fiber consists of a series of links, such that when one link fails the entire fiber fails. The probability of a link failing, $P(\sigma_f)$, is dependent on the presence of a critical flaw. If the flaws do not interact, then each link fails independently of any other link in the fiber. The probability of a fiber surviving is the product of the probabilities of each fiber link not containing any critical flaws. The probability of the fiber failure is given by one minus the probability that the fiber survives. Therefore, the cumulative probability that at least one link breaks at a given stress level, σ_f, is

$$P_f(\sigma_f) = 1 - \left[1 - P(\sigma_f)\right]^N \tag{1.1}$$

where N is the number of fiber lengths and $P_f(\sigma_f)$ is the cumulative distribution function (CDF) for the fiber strength.

Coleman postulated that the probability of fiber failure has the form of the Weibull distribution. Application of the Weibull model (Weibull, 1951) to represent the fiber strength distribution requires several assumptions. First, a fiber that does not fail under a given stress must not fail under a slightly larger stress due to more than one critical flaw. Flaws on the surface of a fiber link are independent of flaws on any other link. Finally, the probability of a critical flaw existing over an infinitesimal stress interval is given by a function of stress, $P(\sigma_f)$. This function must be a non-decreasing function so that the probability of a critical flaw is always greater at higher stress levels.

As a result, Coleman was able to express the probability of fiber failure for long fibers of length L ($N \to \infty$) at or below the stress level σ_f as

$$P_f(\sigma_f) = 1 - \exp\left[-L\left(\frac{\sigma_f}{\sigma_0}\right)^{\beta}\right] \tag{1.2}$$

where σ_0 is the scale factor and β is the Weibull modulus. The probability distribution function (PDF) is calculated by taking the derivative of the CDF in Eq. (1.2):

$$\frac{dP_f}{d\sigma_f} = p_f(\sigma_f) = L\sigma_0^{-\beta}\beta\sigma_f^{\beta-1}\exp\left[-L\left(\frac{\sigma_f}{\sigma_0}\right)^{\beta}\right]. \tag{1.3}$$

Following Coleman, the mean fiber strength $\overline{\sigma}_f$ and standard deviation, s, are expressed

$$\overline{\sigma}_f = \sigma_0 L^{-1/\beta}\Gamma\left(1+\frac{1}{\beta}\right) \tag{1.4a}$$

$$s = \sigma_0 L^{-1/\beta}\left[\Gamma\left(1+\frac{2}{\beta}\right) - \Gamma^2\left(1+\frac{1}{\beta}\right)\right]^{1/2} \tag{1.4b}$$

where Γ is the Gamma function.

The Weibull modulus, β, determines the shape of the distribution. Changes in the shape of the probability density function for four values of the Weibull modulus are plotted in Fig. 1.3. As the Weibull modulus increases, the probability of failure is more concentrated around the mean stress. Typical values of the Weibull modulus are β=4 for graphite fibers, β=10 for glass fibers, and β=20 for ductile metals.

The Weibull modulus is extracted from experimental data by plotting the cumulative distribution on logarithmic axes. The probability of fiber survival, P_s, is equal to

$$P_s = 1 - P_f. \tag{1.5}$$

Substituting into Eq. (1.2) and taking the logarithm yields

$$\ln(P_s) = -L\left(\frac{\sigma_f}{\sigma_0}\right)^{\beta}. \tag{1.6}$$

Taking the logarithm again produces

$$\ln\left(-\ln(P_s)\right) = \ln(L) + \beta\ln(\sigma_f) - \beta\ln(\sigma_0). \tag{1.7}$$

Hence, the Weibull modulus is found by plotting $\ln(-\ln(P_s))$ against $\ln(\sigma_f)$ and calculating the slope. The scale factor, σ_0, is determined from the intercept.

1.4 Strength of glass fiber bundles

A significant decrease in fiber strength is observed when a monofilament is placed in a bundle due to surface flaws induced by contact abrasion between the fibers. Thomas (1971, 1972c) reported that the strength of glass fibers in a bundle reached only 30% of the strength of glass monofilaments. When modeling bundle strength, the fibers in the bundle are assumed unbroken, separated from each other, and subject to the same elongation. As the bundle is loaded, the weakest fibers break in succession and the load is transferred to the unbroken fibers. The breaking load of the bundle occurs when the stress on the remaining fibers reaches the ultimate stress and complete fracture occurs. The ratio of bundle strength to mean fiber strength depends on the Weibull modulus of the fiber strength and is given by

$$\frac{\sigma_b}{\bar{\sigma}} = \left(\frac{1}{\beta e}\right)^{1/\beta} \frac{1}{\Gamma\left(1+1/\beta\right)}. \tag{1.8}$$

The bundle strength is always less than the mean strength of the fibers because the ratio in Eq. (1.8) is always less than unity as shown in Fig. 1.4.

1.4.1 Statistical models

Models to predict the strength of glass fiber bundles have been formulated by Coleman (1958), Phoenix (1974), and others. However, these models are complicated and difficult to apply to experimental data. Bundle failure, unlike individual fiber failure, does not follow the Weibull distribution. Other methods have been reported to extract single fiber statistics from bundle failure.

Both Coleman (1958) and Cowking (1991) applied the Weibull model for single filament failure to fiber failure within a bundle. To determine the Weibull modulus from experimental bundle data, the probability of fiber survival is set equal to the percent of unbroken fibers:

$$1 - P(\sigma_f) = \frac{N}{N_0}. \tag{1.9}$$

Combining Eqs. (1.2) and (1.9) yields

$$1 - P(\sigma_f) = \exp\left[-L\left(\frac{\sigma_f}{\sigma_0}\right)^{\beta}\right] = \frac{N}{N_0}. \tag{1.10}$$

Taking the natural logarithm of Eq. (1.10) twice and simple manipulations lead to the following expressions:

$$L\left(\frac{\sigma_f}{\sigma_0}\right)^{\beta} = -\ln\frac{N}{N_0} \tag{1.11a}$$

$$\ln\left[L\left(\frac{\sigma_f}{\sigma_0}\right)^{\beta}\right] = \ln\ln\left(\frac{N_0}{N}\right) \tag{1.11b}$$

$$\beta\ln(\sigma) + \beta\ln(\sigma_0) + \ln(L) = \ln\ln\left(\frac{N_0}{N}\right). \tag{1.11c}$$

The Weibull modulus is calculated by plotting $\ln(\sigma_f)$ versus $\ln(\ln(N_0/N))$ and taking the slope. The scale parameter σ_o is proportional to $L^{-1/\beta}$ (Cowking 1991).

Ema et al. (1984) and Cowking et al. (1991) presented an acoustic emission (AE) technique to detect the individual fiber breaks throughout the failure of a bundle. The time and load was recorded for each individual break. The stress and percent of

unbroken (surviving) fibers were calculated and then used to construct the Weibull plot (Eq. (1.11c)).

1.4.2 Influences on glass fiber bundle strength

Thomas (1971, 1972a, 1972b, 1972c) carried out an extensive series of experiments to investigate the influence of surface treatment, fiber diameter, gage length, and strain rate on glass fiber bundle strength. The tensile strength was found to decrease with increasing fiber diameter and gage length. Thomas concluded that the increased surface area of larger diameter fibers increased susceptibility to surface damage, and longer gage lengths had a higher probability for critical flaws. The tensile strength was also found to decrease with decreasing strain rate. An increase in bundle tensile strength was reported for several types of surface treatment. Thomas applied different wax and polyester coatings to the bundles. The strength of wax coated bundles increased as much as 59% while the strength of the polyester coated fiber bundles increased as much as 90%. Thomas attributed the increase in strength to a reduction in contact abrasion and an increase in load transfer due to the coating. In more recent studies, Hill and Okoroafor (1995) measured a 14% increase in tensile strength for glass fiber bundles coated with a lubricating oil. Dibenedetto and Lex (1989) coated single glass filaments with a silane surface treatment and observed increases in strength of approximately 18%.

Surface treatments can also be used to protect against environmental corrosion. Humidity aging was also investigated by Dibenedetto and Lex (1989) for individual fibers with and without a silane surface treatment. The fibers treated with silane showed

a dramatic benefit after two hours in boiling water compared with fibers having no surface treatment. Cameron (1968) also investigated the effects of a humid environment. Fiber bundles were conditioned at high humidity (80–100% RH) for 120 days. The strength of the conditioned fibers was approximately 85% of the strength before the humidity conditioning. Cameron also showed that a high temperature (273°C) environment could reduce the fiber strength 40%. A much smaller drop of 3% was observed for bundles conditioned at a lower temperature 100°C. A combination of a high humidity and high temperature environment (100% RH and 90°C) showed a drop in strength to approximately 75% of the non-conditioned strength.

1.5 Overview of thesis

This thesis investigates the influence of surface treatment and humidity on the tensile strength of E-glass, and presents experimental data for E-glass fiber bundles. Four types of commercial surface treatment were tested at four levels of humidity. Acoustic emission sensing was used to detect the individual fiber breaks throughout a bundle tensile test. The AE data were then used to calculate the Weibull modulus for the fibers in the bundle. Chapter 2 describes the test matrix, experimental apparatus, and data reduction procedure. Results of the bundle tests for each surface treatment at each level of humidity are discussed in Chapter 3. The results of a moisture reversibility study and the effects of oven drying are also presented in this chapter. Chapter 4 addresses the issue of twist in the bundle. Tensile results are presented for bundles with different amounts of twist. Finally, conclusions and future work are summarized in Chapter 5.

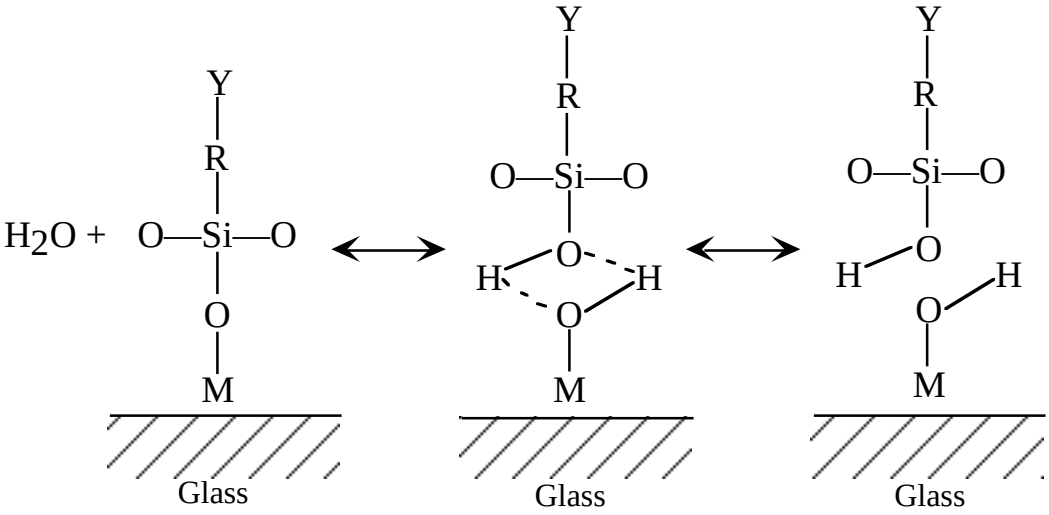

Fig. 1.1. Sample reaction of silane coupling agent with water.

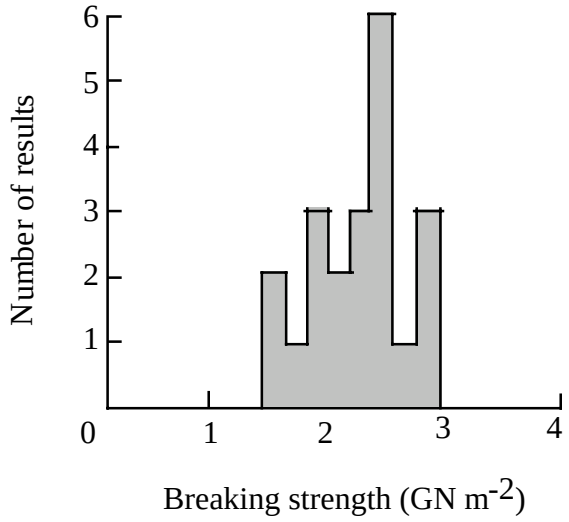

Fig. 1.2. Histrogram of break strength for fibers in a bundle (Hull, 1981).

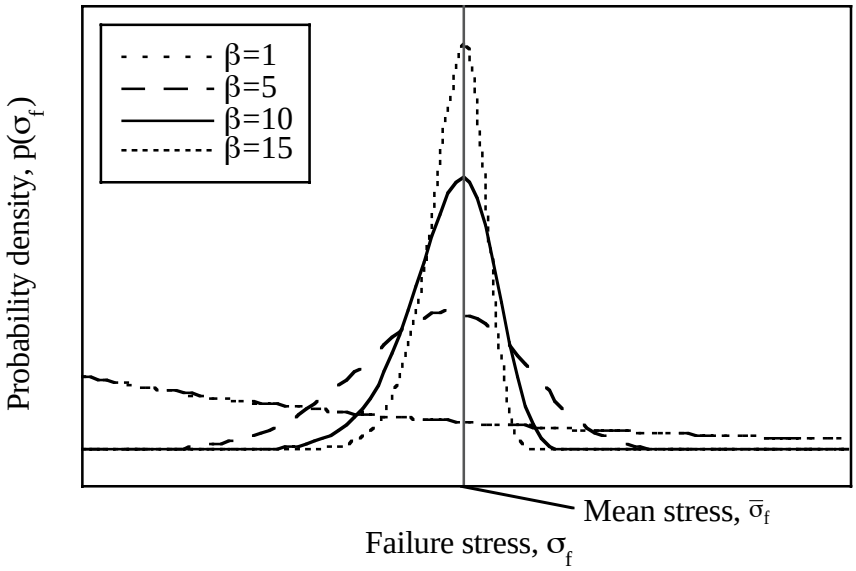

Fig. 1.3. Plot of the probability density for different values of the Weibull modulus, β.

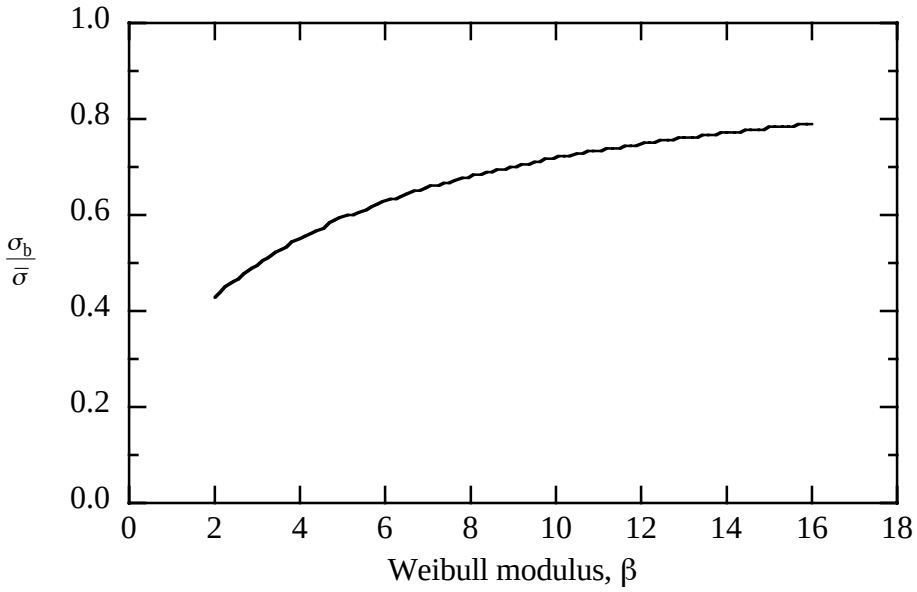

Fig. 1.4. Ratio of bundle strength to average fiber strength as a function of the Weibull modulus.

Chapter 2

Experimental Procedure

2.1 Overview

As mentioned in Chapter 1, the tensile break strength of fibers has been investigated extensively. Most of these previous studies focused on testing single glass filaments rather than bundles and did not consider the effects of any commercial surface treatments or coatings applied to the fiber. In the current work, a series of commercial glass fiber bundles with 204 individual filaments was tested to failure to assess the effects of four different surface treatment on tensile failure after exposure to environments of varying humidity. The effects for different amounts of twist in the bundle were also investigated. Use of an acoustic emission sensor during the test enabled data to be extracted for individual fiber breaks within the bundle. An extensive experimental test matrix was carried out to measure the peak tensile load, strain to failure, and number of fiber breaks at peak load for each of the different bundle types subjected to different RH levels. Weibull modulus and mean fiber strength were determined from individual break data.

2.2 Test matrix

Commercial E-glass fiber bundles were provided by Owens-Corning. Each bundle consisted of 204 individual G150-type filaments with a nominal diameter of nine microns (Owens-Corning 1984). Four different surface treatments, listed in Table 2.1, were chosen for the study. Type I had a starch surface treatment, which is typically placed on the fiber during manufacturing. Type II and III also had the starch surface treatment

applied; however, type II had an added silane and type III had an added wax component. Type IV had no starch, but was treated with an epoxy size.

All four types of fiber bundle were conditioned at four different humidity levels: 10%, 40%, 80% and 100% (fully saturated). Type II samples were placed in an oven at 130°C to determine if the strength would change significantly after a post-bake of the silane. A moisture reversibility study was completed for type I bundles by soaking the bundles for 24 hours, then testing after 1, 24, or 48 hours in a 10% RH environment. Several levels of twist were also tested for type I bundles: zero, one, two, three and five turns per inch.

Table 2.1. Summary of fiber surface treatments.

Type	Surface Treatment	Trade Name
I	Starch	636
II	Starch + silane	646
III	Starch + wax	600
IV	Epoxy	603

2.3 Sample preparation

A typical sample for tensile testing is shown in Fig. 2.1. Samples were fabricated by cutting six-inch lengths of fiber directly from bobbins supplied by Owens-Corning. Before being wound onto the bobbins, 0.7 turns per inch of twist was placed in the bundles by the manufacturer. This twist was removed prior to making the samples. The cut bundle was clipped to a horizontally suspended wooden rod and placed under a hood to prevent movement due to air circulation. Another binder clip was placed on the free end of the bundle and allowed to oscillate until all twist had been removed. The amount

of force on the fiber from the clip was approximately 0.8 N, which was a low enough load that no fiber breaks occurred.

A 25 mm gage length of fibers was chosen because of the lower variation of strength found in shorter samples (Thomas 1971). Silicone rubber molds were made to ensure that gage length was 25 mm—see Fig. 2.2. End tabs (25 mm x 50 mm) were cut from perforated fiberglass circuit boards. Two tabs were placed in the mold, and epoxy was spread onto the surface of the tabs. Untwisted bundles were then laid across the mold. The molds were placed on a bench so that the binder clips could hang over the mold to keep the bundle under a uniform tension; see Fig. 2.3. The end tabs were coated with a highly viscous epoxy and two more tabs were placed on top of the bottom tabs, sandwiching the bundle between them. Toothpicks were cemented between the two sets of tabs to hold the bundle straight and make handling easier. After a 24 hour cure, the specimens were placed into an oven or humidity chamber.

2.4 Environmental conditioning

To obtain different humidity levels, a plexiglass chamber was constructed (Fig. 2.4). A 4-inch diameter, round opening was cut into the top for access and sealed with an O-ring. Low RH values (10, 40%) were obtained with a vacuum pump that pumped air out of the chamber, through a desiccant column, and then back into the chamber. A timer was used to maintain the desired humidity level. The higher, 80% RH environment was created in the chamber using a modified warm-air room humidifier. A plastic funnel was attached such that the large diameter of the funnel was over the humidifier and the small

diameter was connected to a hose leading into the chamber. The hose was always elevated so the warm, moist air would flow into the chamber. A dial setting on the humidifier was used to maintain the desired humidity level. The 100% saturation condition was obtained by soaking the fiber bundles in distilled water for 24 hours. A set of type II fibers was also post-baked in an oven at 130°C. After 48 hours in the oven, the samples were placed in either a 40 or 100% RH environment.

2.5 Experimental apparatus

An Instron Mini 44 with a 500 N load cell was used to perform the tension test. A specimen was removed from the humidity chamber and placed between the rubber faced grips. Figure 2.5 shows the entire tension test set-up.

A small compressive load was first placed on the specimen so that after the toothpicks were cut, a tensile load would not be suddenly applied to the bundle. The load was then balanced and a small pre-load of approximately 1 N was applied. The crosshead displacement was set to zero at this point. A LabVIEW program was used to control the Instron and acquire load–displacement data. A constant displacement rate of 0.05 mm/min was used for all tests.

Individual fiber breaks were recorded during tensile testing of the bundle with the aid of a standard acoustic emission (AE) setup, shown schematically in Fig. 2.6. A 150 kHz piezoelectric AE sensor (Dunegan, SE 150-M) was fixed to the sample end tab with a small C-clamp; see Fig. 2.7. The signal from the sensor was amplified (Dunegan, 400p-

100) and then recorded by a 400 MHz oscilloscope (LeCroy, Model 9310). The threshold voltage was set at 0.5 V to trigger the scope. An individual fiber break created an AE signal similar to that shown in Fig. 2.8. The entire waveform, as well as the time of the break relative to the start of the test, were recorded. The voltage output from the load cell was also stored. The oscilloscope was set to record a maximum of 205 signals: 204 fibers in the bundle and one initializing signal from the power source, caused by the initial movement of the crosshead. Hence, the failure load of each individual fiber was measured during a single bundle test.

The test was run until all fibers in the bundle were broken. After the test was completed, the load and time of break were transferred from the oscilloscope to a computer via an RS232 connection. Load–displacement data were recorded via LabVIEW on a separate computer. The LabVIEW program and the oscilloscope were then reset for the next test.

2.6 Data reduction

Bundle strains were calculated directly from crosshead displacement and the known gage length. A typical load–strain plot is shown in Fig. 2.9. The solid line represents the load–displacement data from the Instron and each data symbol represents an individual fiber break detected by the AE sensor. The peak load, the number of breaks recorded before the peak load, and the strain at failure were recorded for each data set. A small nonlinear region in the load–displacement curve due to machine and fixture compliance was observed in all tests. After 0.5% strain or a load of approximately 2 N, the

load–displacement curve was linear until the first fiber break, as shown in Fig. 2.9. The load continued to increase after the first break until reaching a critical point, followed by rapid failure.

The statistical behavior of individual fiber breaks was analyzed using the method presented by Cowking (1991) and described in Section 1.4.1. The stress in the surviving fibers after each break was calculated by

$$\sigma = \frac{P}{\pi (r_f)^2 N_s} \tag{2.1}$$

where P is the load, r_f is the radius of each filament and N_s is the number of surviving fibers. A Weibull plot is created by plotting $\ln(\sigma)$ versus the $\ln(\ln(N_0/N))$. The slope of this curve is the Weibull modulus, β, while the intercept is the Weibull scale parameter, σ_0. A typical Weibull plot is shown in Fig. 2.10. Above a certain value of $\ln(\ln(N_0/N))$, the plot becomes nonlinear. Near the end of the test, many breaks occur simultaneously and some are not recorded by the oscilloscope. An inaccurate calculation of stress via Eq. (2.1) results. The inaccuracy in the stress values causes the Weibull plot to flatten out as ln ln (N_0/N) increases. The data above the line in Fig. 2.10 are not valid and are not used to determine the slope. The Weibull modulus is calculated in a similar fashion for each bundle test and then averaged for each data set. A higher Weibull modulus indicates a distribution of fiber breaks closely centered around the average breaking strength.

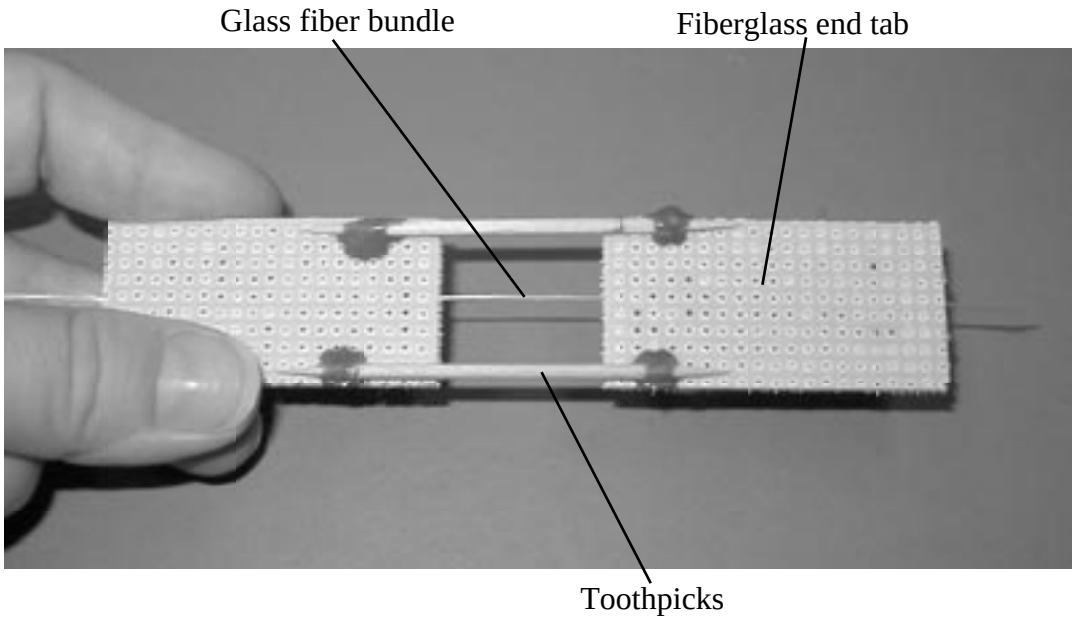

Fig. 2.1. Finished glass fiber bundle tensile specimen.

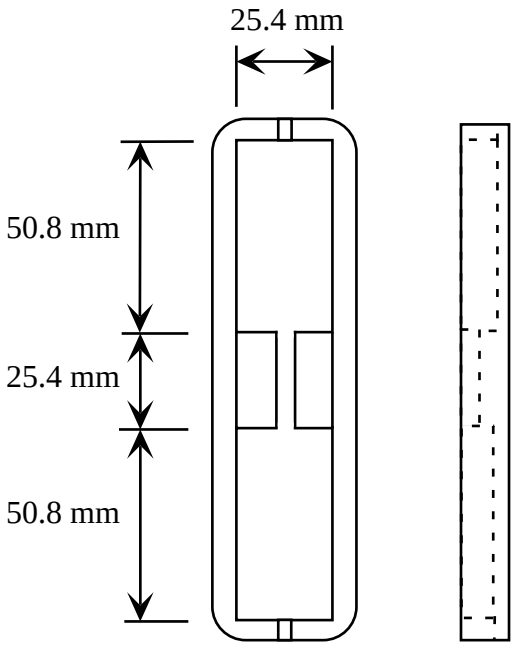

Fig. 2.2. Silicone rubber mold.

Fig. 2.3. Glass fiber in mold on bench.

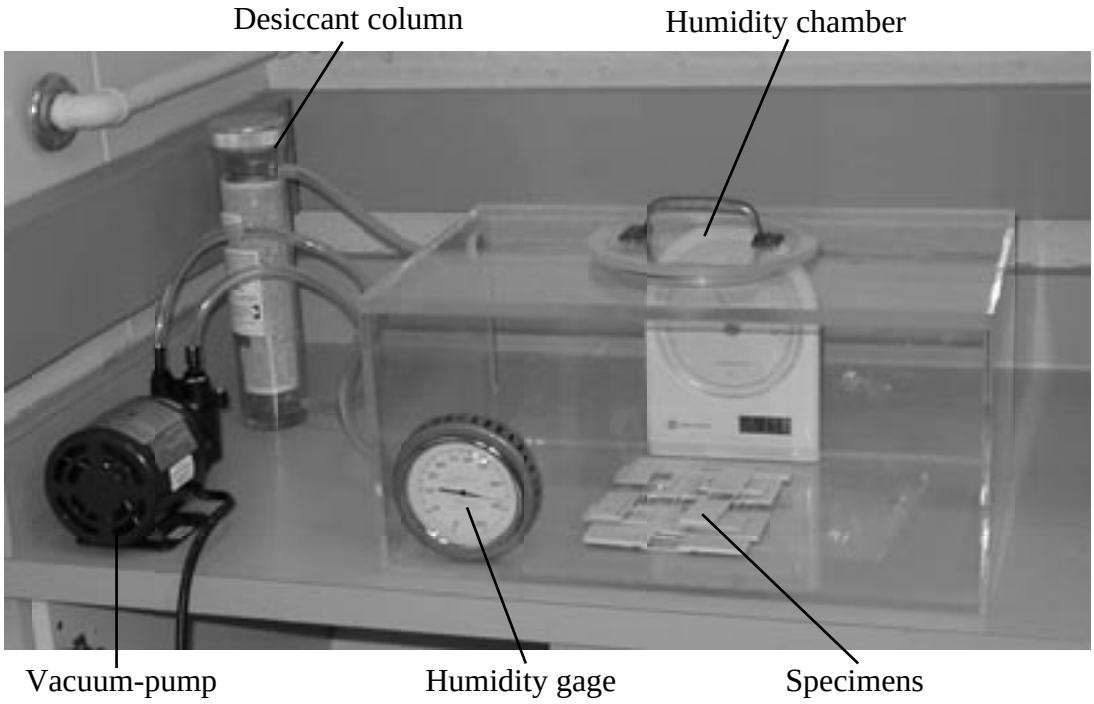

Fig. 2.4. Humidity chamber connected to vacuum-pump and desiccant column.

Fig. 2.5. Tension test setup.

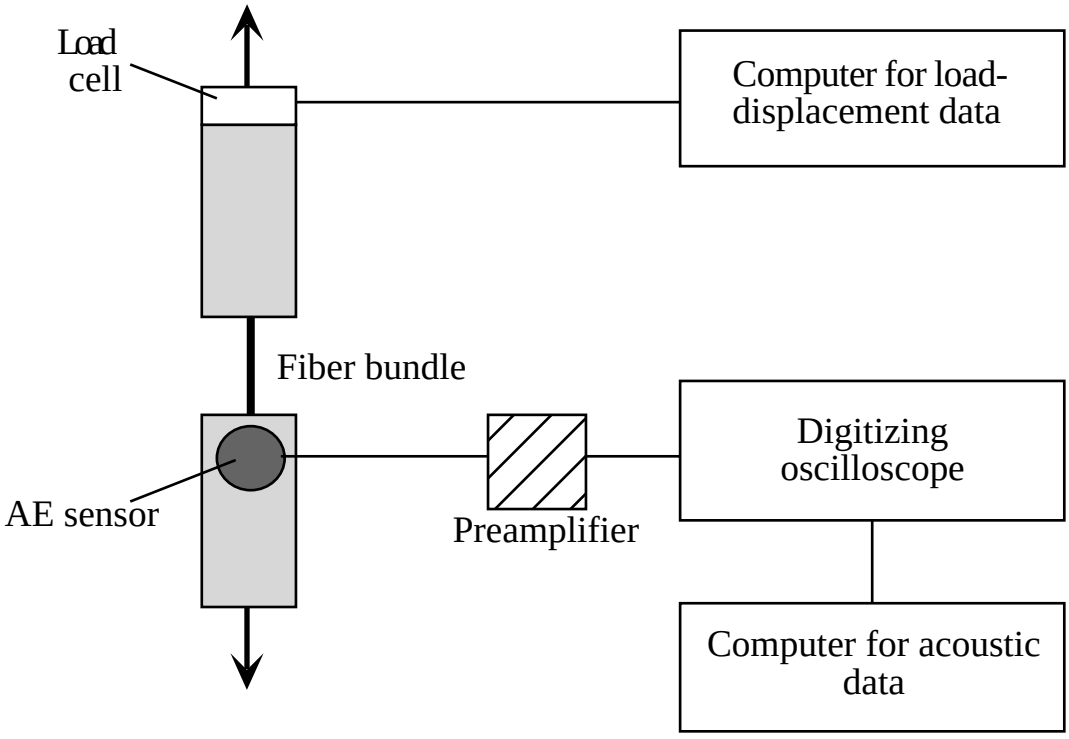

Fig. 2.6. Schematic of test setup.

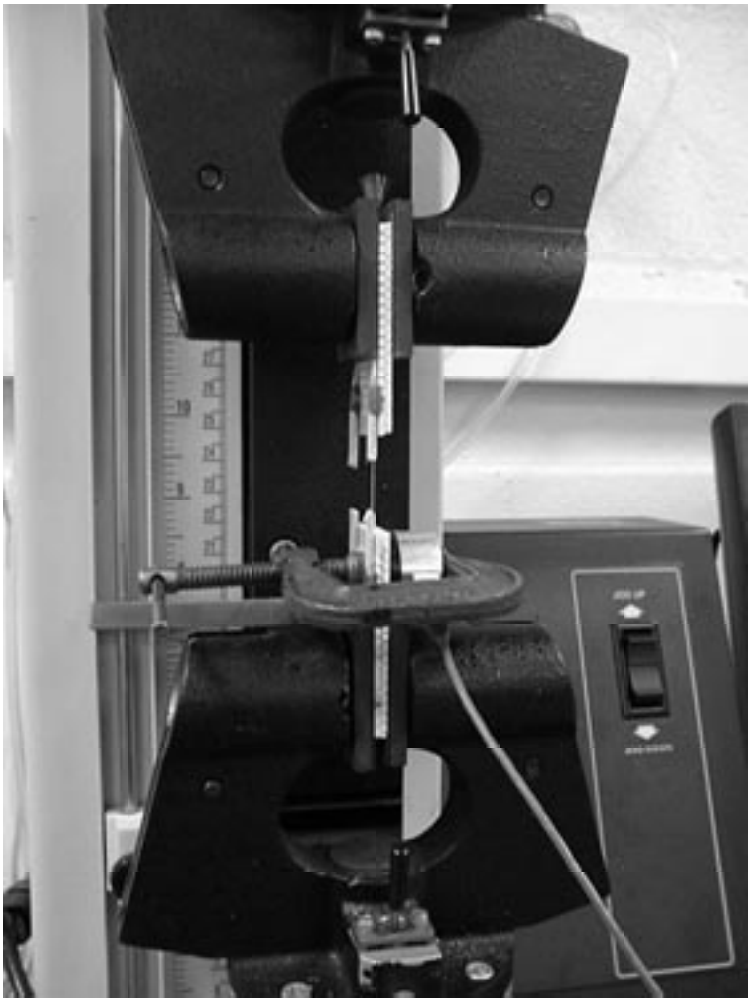

Fig. 2.7. AE sensor attached to specimen.

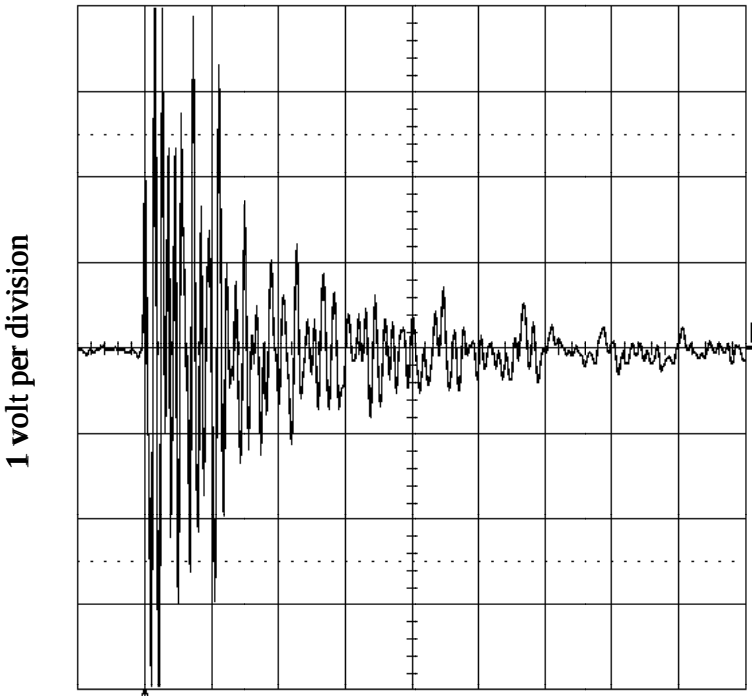

Fig. 2.8. Typical waveform recorded by oscilloscope.

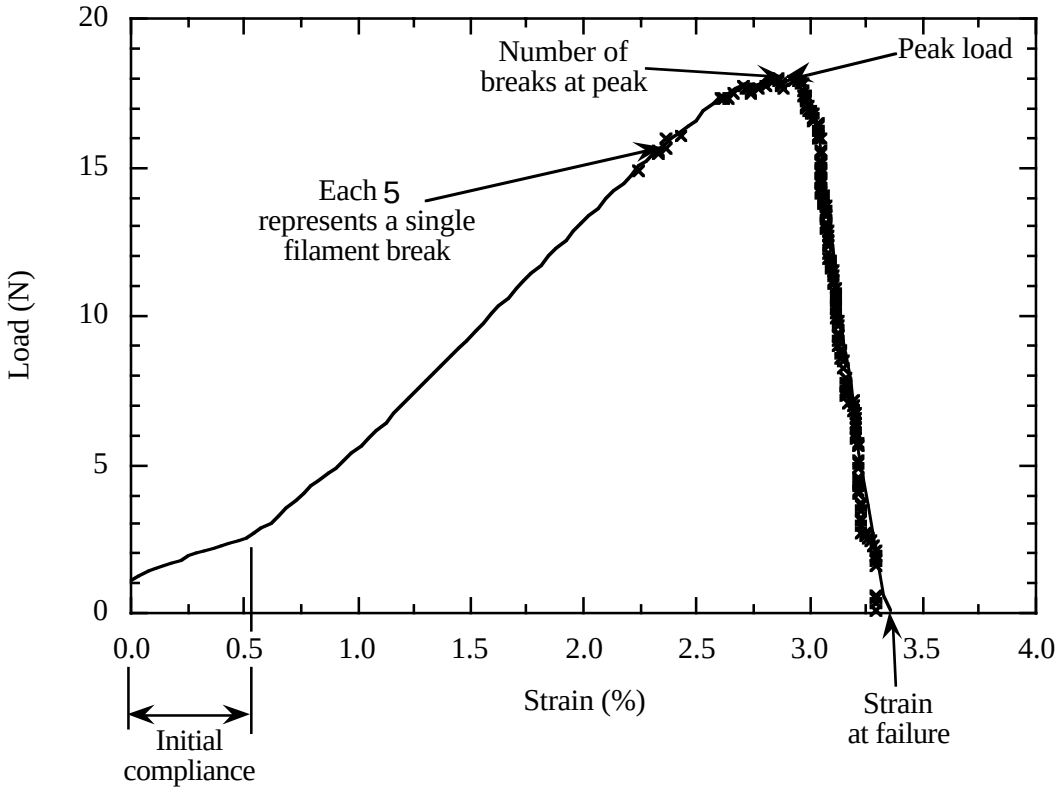

Fig. 2.9. Typical load–strain plot.

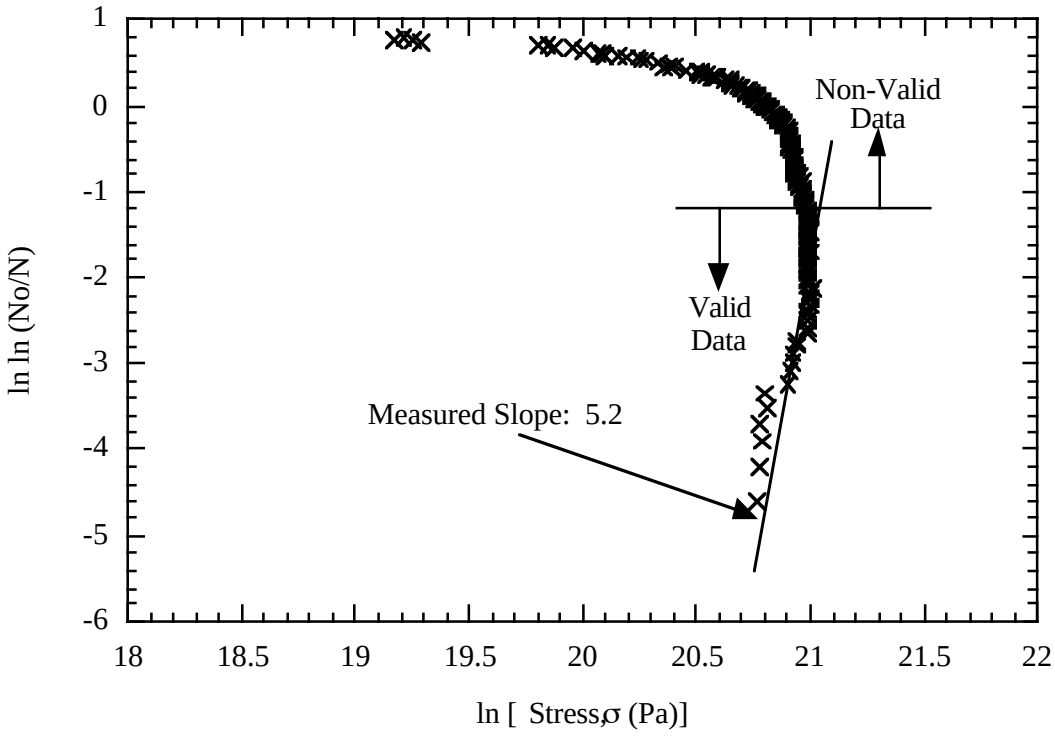

Fig. 2.10. Typical Weibull plot.

Chapter 3

Effects of Humidity Aging

3.1 Overview

The four types of fiber bundles (Table 2.1) were tested after conditioning in four different levels of humidity: 10, 40, 80, and 100% RH. Twenty samples were tested for each combination of surface treatment and humidity level, and the average and standard deviation of each data set were calculated. The data for each of the different surface treatments were compared at each humidity level. A moisture reversibility study was also performed using a smaller set of type I bundles. The samples were first soaked at 100% RH for 24 hours, then dried out at 10% RH and tested after 1, 24,and 48 hour increments. The effect of oven-drying the silane treated fibers (type II) was also investigated. Summaries of the averages and standard deviations for all the data sets are listed in Tables 3.1 to 3.6. The data recorded for individual tests are given in the Appendix.

3.2 Starch surface treatment

Type I fibers have a starch based surface treatment. The starch size aids in winding the bundles onto bobbins for storage by preventing static and providing lubrication between the fibers. Representative load–strain curves for type I fiber bundles are plotted in Fig. 3.1 and the average data obtained for all type I samples are listed in Table 3.1 for each humidity level. The 10%, 40%, and 80% RH curves have similar average peak loads and number of fiber breaks at the peak load. The strain to failure of the 10% RH treated bundles is slightly larger than that of the bundles treated at 40% RH, while the strain to failure is much larger for the 80% RH bundles. A noticeable difference is observed between the 100% RH curve and the lower humidity curves. The average peak load is much lower and the number of breaks at peak load is much higher than the other sets of data. However, the shape of the curve and the strain at failure are similar to those at the lower humidity levels.

A typical Weibull plot for type I bundles conditioned at each humidity level is shown in Fig. 3.2. The Weibull data contained a considerable amount of scatter for many of the tests, making it difficult to identify a linear region. The Weibull modulus of the 10% RH data is much larger than that of the 40%, 80%, and 100% RH data. Due to the scatter in the data, the standard deviations of the Weibull moduli are fairly large except for the 40% RH level.

3.3 Silane and starch surface treatment

Type II bundles have a silane added to the type I starch chemistry, which can protect against moisture damage. Figure 3.3 contains representative load–strain curves for type II bundles at each humidity level, and a summary of all type II tensile data is given in Table 3.2. Again, samples conditioned at the 10%, 40%, and 80% humidity levels have a similar average peak load, while the samples conditioned at 100% RH have a lower average peak load. The bundles conditioned at low (10% and 40% RH) humidity fail almost instantaneously after reaching peak load. Samples conditioned at the higher humidity levels (80% and 100% RH) have a more rounded peak, indicating a slower failure of the bundle. Again, the 80% RH sample had the largest strain to failure. The number of breaks at the peak is consistent for each humidity level.

A typical Weibull plot for individual filaments in a single bundle is shown in Fig. 3.4. For type II, the average Weibull modulus increases for each increase in humidity except at 40% RH, which is slightly lower than the other humidity levels. The standard deviations for 80% and 100% RH are very large.

3.4 Wax and starch surface treatment

Type III bundles have a wax added to the type I starch chemistry, which functions as a lubricant between the fibers. The wax reduces the damage due to frictional sliding between fibers and can aid in the weaving of fiber bundles. Typical load–strain curves for the type

III fiber bundles are shown in Fig. 3.5 and all the data are summarized in Table 3.3. As for the type I and type II bundles, the average peak loads for 10%, 40%, and 80% RH conditioned samples are similar. However, the average peak load for 100% RH data is significantly lower. All the type III load–strain curves are more rounded near the peak load compared with the previous data. This result indicates slower failure of the bundles and implies a greater scatter in the individual filament strengths. This scatter is also apparent in the large number of breaks recorded before the peak load. The failure strains are similar at all levels of humidity for this bundle type.

Figure 3.6 shows representative Weibull plots for the type III bundles. The Weibull moduli calculated for the type III bundles are much lower than those of the type I and type II samples for all humidity levels. A lower Weibull modulus implies a greater scatter in breaking strength for the individual fibers in a bundle, which is also indicated by the load–strain data.

3.5 Epoxy surface treatment

Type IV fiber bundles had a significantly different surface chemistry than types I, II, and III. These bundles had an epoxy size placed on them during drawing. The epoxy is used to enhance interfacial adhesion between the bundle and an epoxy matrix after embedding. Because of the epoxy size, the surface roughness of the fibers is higher than that of the type I fibers. The load–strain curves for type IV bundles in Fig. 3.7 show no significant changes with humidity level. All the tensile data for type IV bundles are summarized in Table 3.4. The average peak load, number of breaks at peak load, and strain to failure are similar at all levels of humidity, including 100% RH.

Representative Weibull plots for type IV bundles are shown in Fig. 3.8. As for the load–strain curves, the type IV Weibull plots are similar in both shape and slope. The

scatter is similar for all the data, and the calculated values of the Weibull moduli at 10%, 40%, and 80% RH levels are nearly the same. The average Weibull modulus for the 100% RH data is higher.

3.6 Comparison of surface treatments

Overall, the type of surface treatment applied to the fibers had the most significant effect on the peak load. The influence of humidity conditioning was secondary and depended significantly on the surface treatment. A comparison of the average peak loads listed in Tables 3.1, 3.2, 3.3, and 3.4 reveals that glass fiber bundles with the type II surface treatment had a consistently higher breaking strength than bundles with the other types of surface treatments at every humidity level. A consistently lower breaking strength was measured for bundles with the type IV surface treatment at 10%, 40%, and 80% RH. Humidity conditioning at 10%, 40%, and 80% had no measurable effect on breaking strength within the scatter of the experiments performed. Conditioning at 100% RH (fully saturated), however, had a much more significant effect.

The bar chart in Fig. 3.9 summarizes the differences in the average peak load for each surface treatment at 10% and 100% RH. At 10% RH, type II bundles had the highest peak load, followed by type III, type I, and type IV with the lowest. A significant decrease in breaking strength was measured for type I, II, and III samples conditioned at 100% RH compared with the value measured for samples conditioned at 10% RH. The drop in peak load was most significant for samples with the type III surface treatment. Only type IV samples showed no significant decrease in breaking strength after conditioning at 100% RH.

The average number of breaks at the peak load is compared in Fig. 3.10 for each surface treatment at 10% and 100% RH. Only 10% and 100% RH data are presented in Fig. 3.10

because no significant difference in the number of breaks at peak load were observed between the 10%, 40%, and 80% RH levels. At 10% RH, types I, III, and IV had an average number of eleven breaks at peak load, while type II had a slightly lower number. The number of breaks at peak increased significantly at 100% RH for type I and type III samples. Type II bundles had only a slight increase in the average number of breaks at 100% RH, while type IV showed a sizable decrease in the average number of breaks at peak.

Figure 3.11 compares the average strain to failure for all surface treatments at 10%, 80%, and 100% RH. The data for fibers conditioned at 40% RH have been omitted from the chart because of the similarity of the 10% and 40% RH data. The failure strains are similar for type I, II, and III bundles conditioned at 10% and 100% RH. However, for the same sample types conditioned at 80% RH, the strain to failure is significantly higher than that at 10% or 100% RH. An adhesive force caused by the surface tension of the water could bind the fibers together and cause some load sharing to take place. The fibers conditioned at 100% RH reach a much lower peak load, so a higher strain to failure cannot be reached even with load sharing. Type IV has lower strains to failure than the other surface treatments at all humidity levels, most likely due to increased contact abrasion from the epoxy size.

The average values of Weibull moduli for each surface treatment are compared in Fig. 3.12. Again, only 10% and 100% RH data are included. At 10% RH, types I, II, and IV have similar Weibull moduli while type III has a slightly lower value. The Weibull modulus increases for types II, III, and IV with 100% RH conditioning. The Weibull modulus for type I bundles does not follow the same trend as the other types and decreases at humidity levels greater than 10% RH.

The silane treated fibers (type II) have the highest average peak load at all humidity levels. Type II bundles also had the lowest number of breaks before the peak load. The silane applied during manufacturing protects the fibers from long-term moisture damage and appears to have the most significant positive effect on the performance of the glass fiber bundles. The silane not only protects against moisture, but also decreases the amount of contact abrasion. In this study, the increase in average peak load for the silane surface treatment was approximately 3% at 80% RH, which is much lower than the 18% increase observed by Dibenedetto and Lex for single glass fibers (1989).

The wax surface treatment reduces contact abrasion, but does not protect the fibers from moisture damage. For low humidity levels, the increase in average peak load was close to 2% when adding a wax surface treatment. The average peak load of type III bundles conditioned at 10, 40, and 80% RH is higher than that of type I bundles and almost as high as that of type II bundles. The average peak load for fully saturated (100% RH) type III bundles drops to the same level as type I bundles, while the peak load does not drop as much for type II bundles. These observations imply that the wax reduces contact abrasion and improves the peak load even when the humidity reaches 80% RH. However, when the wax treated fibers are conditioned at 100% RH, the wax no longer effective and moisture damage dominates.

The fibers with an epoxy size (type IV) did not have a significant change in average peak load at any humidity level. Direct comparison with types I, II, and, III should be avoided because type IV fibers are not treated with a starch chemistry prior to the epoxy size. However, it is interesting to note that the average peak load for type IV fibers conditioned at each humidity level is close to the value for type I fibers at 100% RH. The epoxy not only allows moisture damage to occur, but may also hold the moisture in the

bundle. The epoxy size also causes more contact abrasion than other surface treatments because the surface is rougher. This rough surface may also cause a lower peak load.

3.7 Fiber diameter measurements

The diameter of glass fibers cannot be precisely controlled, and a distribution of diameters is found for fibers in a bundle. The scatter in diameters is observed at a cross-section as shown in Fig. 3.13. Not only is scatter seen at a single cross-section, but also each monofilament may have a non-uniform diameter along the length of the fiber. A series of tests were run until two or three fibers had broken. The test was halted, then the sample was unloaded and removed from the test frame. The diameters of the broken fibers were then measured using an optical microscope. A group of approximately 20 unbroken fibers were also recorded for comparison. Three specimens were tested and measured for each surface treatment type. Table 3.7 shows the average diameters for the first fiber breaks and the non-broken fibers. The average diameter for the first few breaks for each surface treatment type is larger than the average unbroken fiber diameter. The data suggest that larger diameter fibers in the bundle are weaker. Thomas (1971) postulated that the decrease in strength with increasing fiber diameter was due to contact abrasion.

Table 3.7. Fiber diameters measured from the first breaks and remaining unbroken fibers.

Surface treatment	Type I	Type II	Type III	Type IV
First break diameters, μm	10.4 ± 0.5	10.2 ± 0.4	10.0 ± 0.6	10.2 ± 0.5
Unbroken fiber diameters	9.2 ± 0.4	9.0 ± 0.4	9.4 ± 0.5	9.2 ± 0.4

3.8 Acoustic emission waveforms

Typical waveforms for types I, II, and III bundles are shown in Figs. 3.14, 3.15, and 3.16. These waveforms are very similar except that the type II signal has a slightly longer duration. Figure 3.17 shows a different type of signal recorded during a tension test of type III bundles. The size and shape of the signal indicate that this waveform is not a fiber break, but may be noise from fiber contact. The waveform for type IV bundles (Fig. 3.18) is different in size and shape than for types I, II, or III. Figure 3.19 shows another type of signal recorded during a tension test of type IV bundles. The difference in size and shape of these waveforms may be caused by the large amount of surface friction due to the epoxy size.

3.9 Reversibility of moisture effects

Type I fiber bundles show a large decrease in strength when aged in a 100% RH environment compared with a 10% RH environment. A reversibility study was carried out to investigate if the strength at 10% RH could be obtained after the fibers had been aged at 100% RH. Type I fibers were first conditioned at 100% RH for 24 hours, then placed in a 10% RH environment for a 1, 24, or 48 hour period. An increase in peak breaking load compared with the type I bundles at 100% RH would indicate if bundle strength can be regained in a low humidity environment.

Representative load–strain curves are plotted in Fig. 3.20 for the different time periods in the low humidity environment and 10% RH only. Average data for all samples are summarized in Table 3.5. A slight increase in strength and strain to failure is measured as the re-conditioning time at 10% RH increases. In Fig. 3.21, the average peak loads are compared for each time interval in the 10% RH environment. A steady increase is shown from 0 to 48 hours at 10% RH. The previously obtained average peak load for 10% RH

conditioning reported in Section 3.2 is included for comparison. The 24 and 48 hour peak loads are approximately equal to the 10% RH peak load, which implies a full recovery.

3.10 Effect of oven drying

The influence of oven drying on the breaking strength of type II bundles was also investigated. Extended oven drying insures a full cure of the silane in the type II surface treatment. A set of type II samples were dried in an oven for 48 hours at 135°C and then conditioned in either a 40% RH or 100% RH environment. The data from the oven-dried and 40% RH conditioned (OD + 40% RH) and the oven dried and 100% RH (OD + 100% RH) samples were compared with the non-oven-dried 40% and 100% RH data reported in Section 3.3.

Typical load–strain curves for the OD + 40% RH and the OD + 100% RH type II bundles are plotted in Fig. 3.22. Average data for all of the samples are listed in Table 3.6. The OD + 40% RH data are quite similar to the non-oven dried 40% RH data presented previously in Fig. 3.4 and Table 3.2. However, there are several interesting differences between the OD + 100% RH data and the non-oven-dried 100% RH data. The OD + 100% RH bundles had a much larger average strain to failure (4.4 ± 0.6%) when compared with the value for 100% RH conditioned bundles (3.8 ± 0.3%). It is interesting to note that the type II bundles conditioned at 80% RH, which was a warm and moist environment, also had a high strain to failure (4.5 ± 0.3%). The average number of breaks at peak load also increased significantly for the OD + 100% RH samples. The average peak load for the OD + 100% RH (17.8 + 2.4 N) was lower than that for the 100% RH samples (21.0 ± 1.9 N). The peak load for bundles conditioned at 40% RH were not significantly affected by the post-bake, but the peak load for bundles conditioned at 100% RH decreased.

Table 3.1. Averages and standard deviations of tensile data for each surface treatment at 10% RH.

Surface treatment	Type I	Type II	Type III	Type IV
Peak load (N)	18.9 ± 1.2	23.9 ± 1.5	22.1 ± 1.3	17.1 ± 2.1
Number of breaks at peak	11 ± 4	8 ± 3	12 ± 5	11 ± 3
Strain at failure (%)	3.6 ± 0.3	4.1 ± 0.3	3.9 ± 0.3	3.1 ± 0.3
Weibull modulus	13.6 ± 3.5	10.6 ± 3.1	4.7 ± 2.4	12.8 ± 2.3

Table 3.2. Averages and standard deviations of tensile data for each surface treatment at 40% RH.

Surface treatment	Type I	Type II	Type III	Type IV
Peak load (N)	18.1 ± 2.0	22.7 ± 2.3	20.7 ± 1.3	18.4 ± 3.6
Number of breaks at peak	13 ± 5	8 ± 4	20 ± 8	7 ± 3
Strain at failure (%)	3.2 ± 0.3	3.5 ± 0.3	3.7 ± 0.3	3.0 ± 0.3
Weibull modulus	6.6 ± 1.6	7.1 ± 1.5	3.6 ± 1.3	14.2 ± 5.2

Table 3.3. Averages and standard deviations of tensile data for each surface treatment at 80% RH.

Surface treatment	Type I	Type II	Type III	Type IV
Peak load (N)	18.6 ± 1.9	24.4 ± 1.3	22.0 ± 2.2	16.5 ± 1.3
Number of breaks at peak	15 ± 6	9 ± 4	14 ± 6	10 ± 4
Strain at failure (%)	4.2 ± 0.5	4.5 ± 0.3	4.2 ± 0.6	3.1 ± 0.1
Weibull modulus	8.5 ± 3.0	14.8 ± 6.3	5.9 ± 2.2	14.2 ± 3.7

Table 3.4. Averages and standard deviations of tensile data for each surface treatment at 100% RH.

Surface treatment	Type I	Type II	Type III	Type IV
Peak load (N)	16.0 ± 1.2	21.0 ± 1.6	16.4 ± 2.0	17.1 ± 1.8
Number of breaks at peak	21 ± 5	9 ± 4	17 ± 5	5 ± 2
Strain at failure (%)	3.8 ± 0.4	3.8 ± 0.3	3.9 ± 0.5	2.9 ± 0.3
Weibull modulus	8.8 ± 2.6	16.9 ± 7.2	8.3 ± 3.6	17.4 ± 7.1

Table 3.5. Averages and standard deviations of tensile data for moisture reversibility data.

Time at 10% RH	1 hour	24 hours	48 hours
Peak load (N)	17.6 ± 0.9	18.5 ± 0.9	19.6 ± 1.6
Number of breaks at peak	10 ± 4	14 ± 5	13 ± 3
Strain at failure (%)	3.2 ± 0.2	3.5 ± 0.2	3.6 ± 0.3
Weibull modulus	11.9 ± 1.7	11.5 ± 2.0	12.0 ± 2.8

Table 3.6. Averages and standard deviations of tensile data for OD + 40% RH and OD + 100% RH.

Humidity level	PB + 40% RH	PB + 100% RH
Peak load (N)	22.9 ± 2.1	17.8 ± 2.2
Number of breaks at peak	9 ± 6	22 ± 3
Strain at failure (%)	3.9 ± 0.4	4.4 ± 0.6
Weibull modulus	12.7 ± 3.4	8.2 ± 5.2

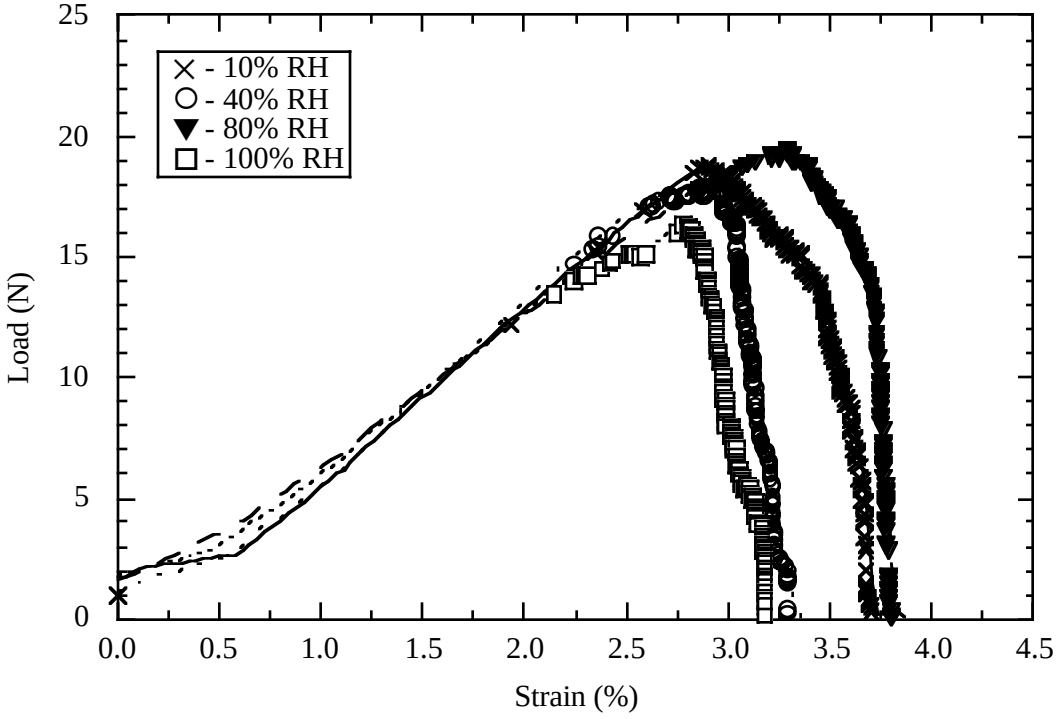

Fig. 3.1. Representative load–strain data for type I bundles at each humidity level.

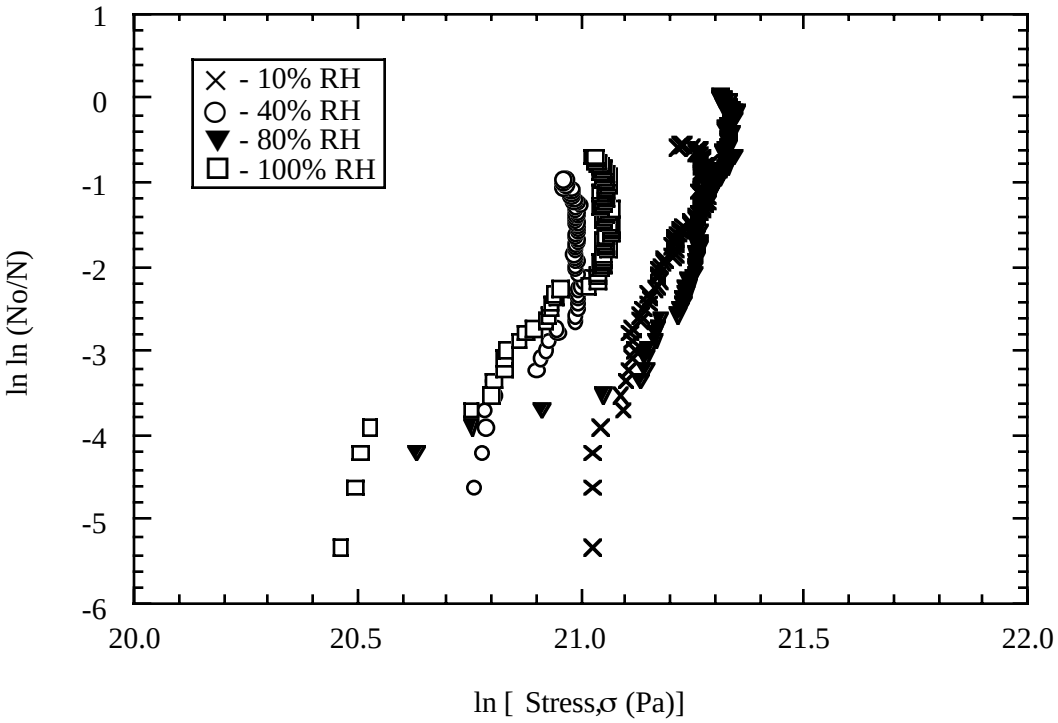

Fig. 3.2. Representative Weibull plot for type I bundles at each humidity level.

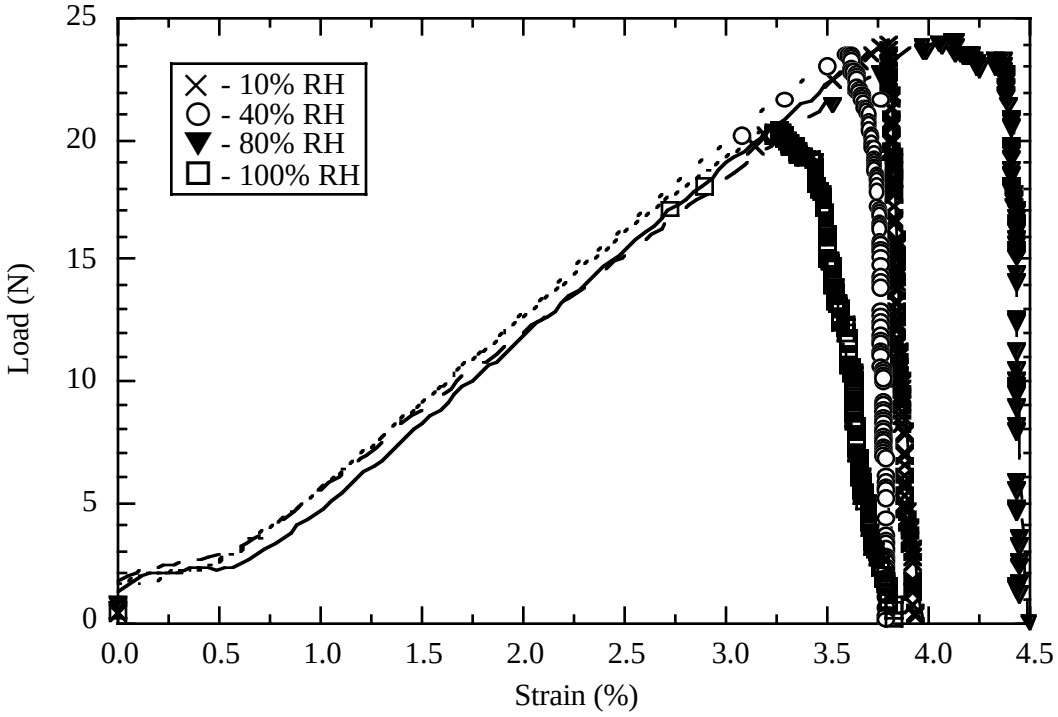

Fig. 3.3. Representative load–strain data for type II bundles at each humidity level.

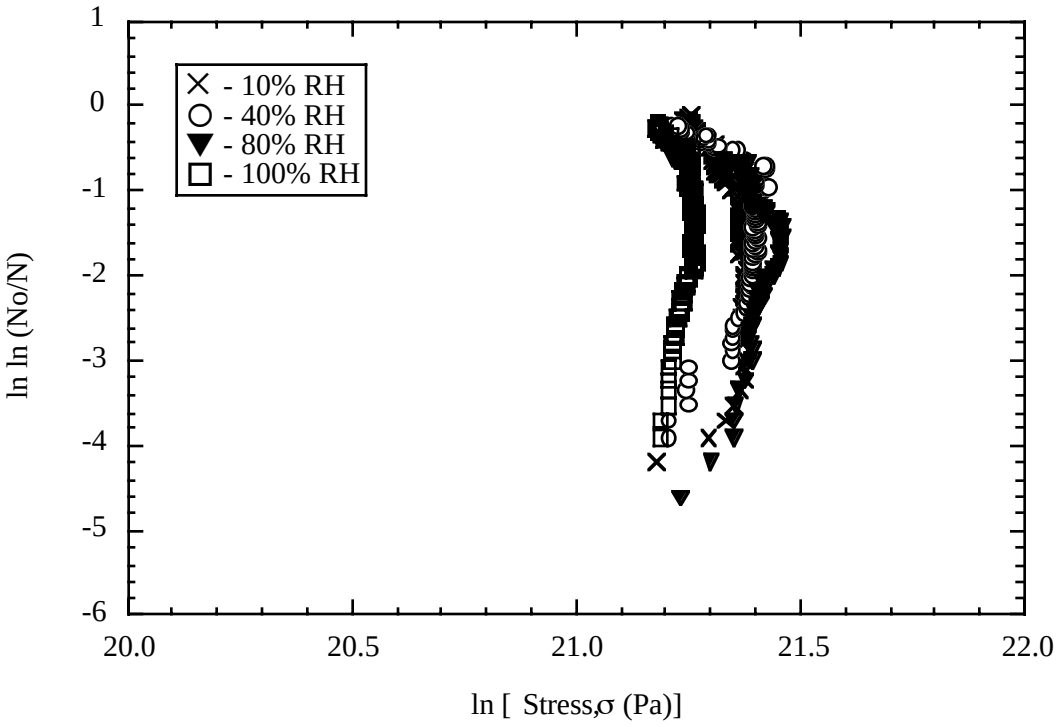

Fig. 3.4. Representative Weibull plot for type II bundles at each humidity level.

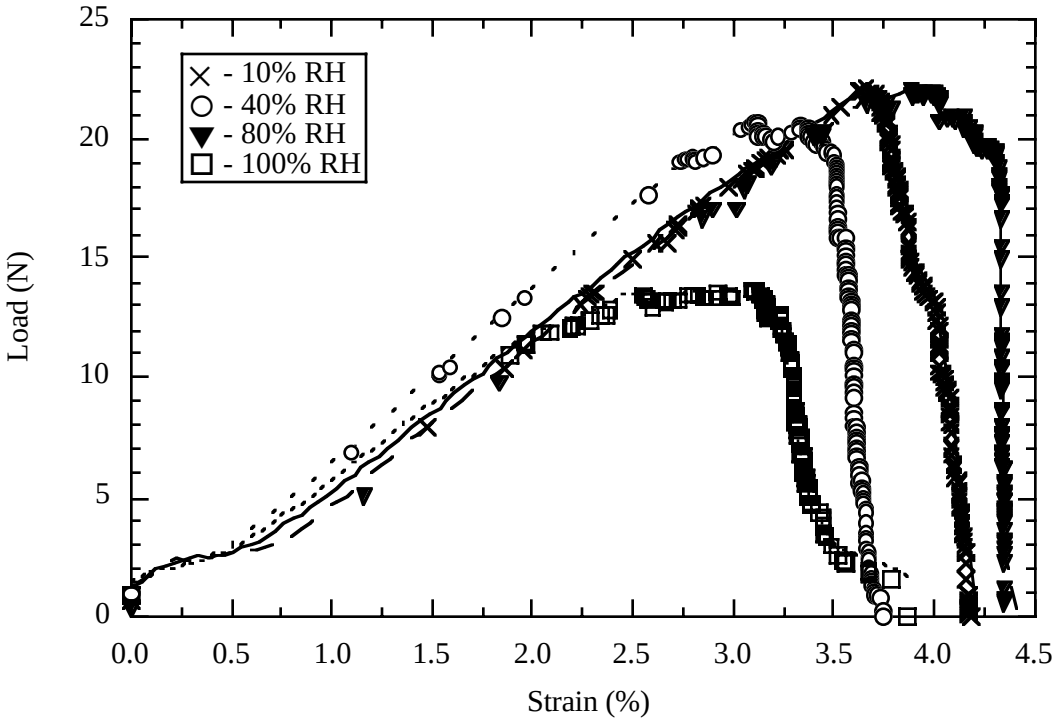

Fig. 3.5. Representative load–strain data for type III bundles at each humidity level.

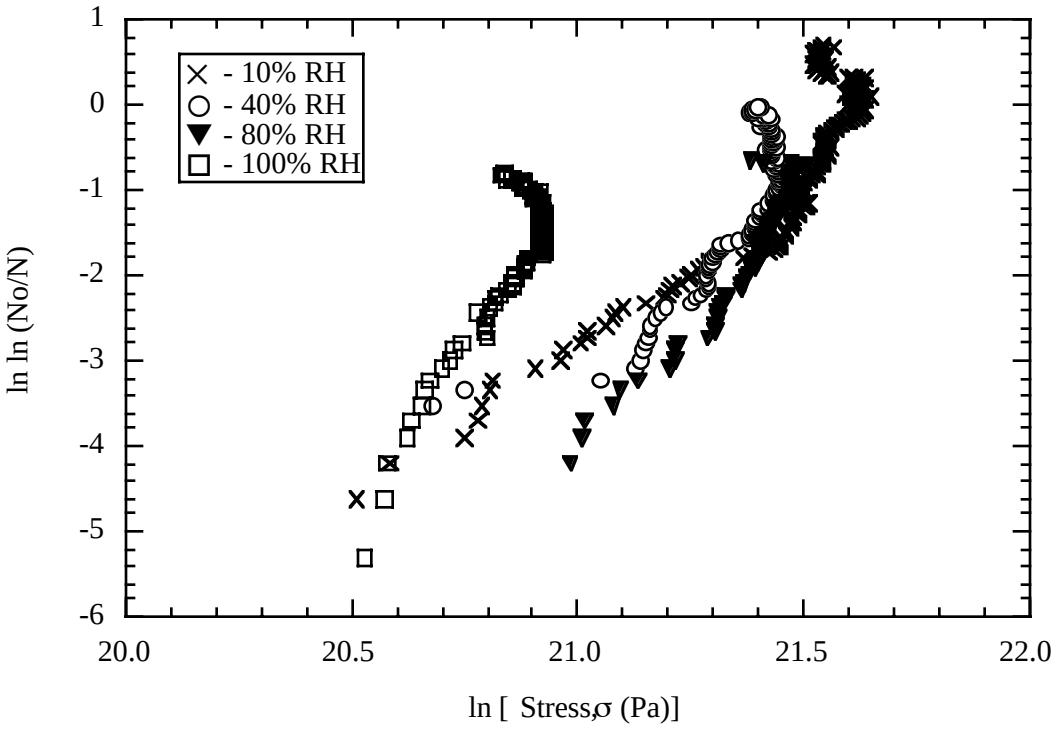

Fig. 3.6. Representative Weibull plot for type III bundles at each humidity level.

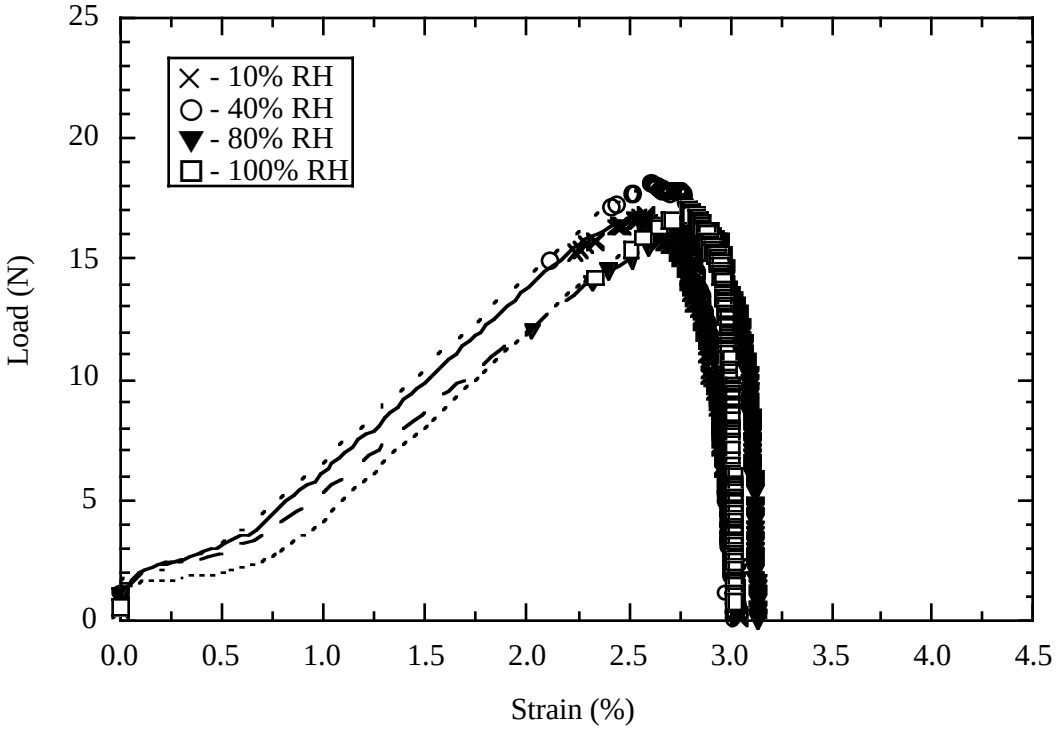

Fig. 3.7. Representative load–strain data for type IV bundles at each humidity level.

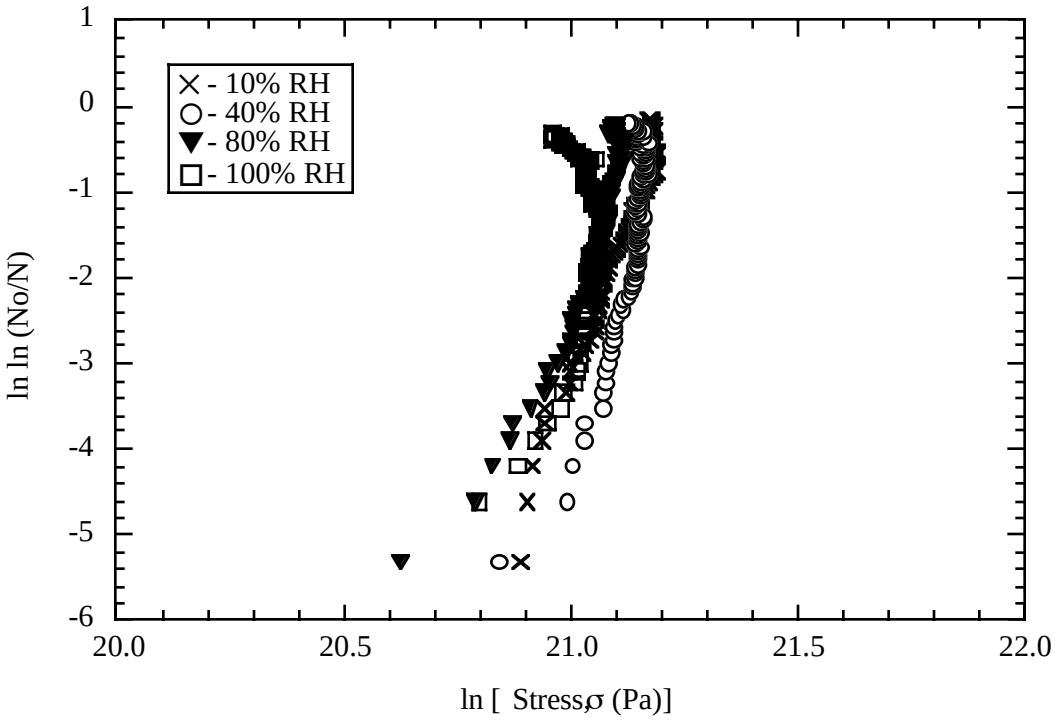

Fig. 3.8. Representative Weibull plot for type IV bundles at each humidity level.

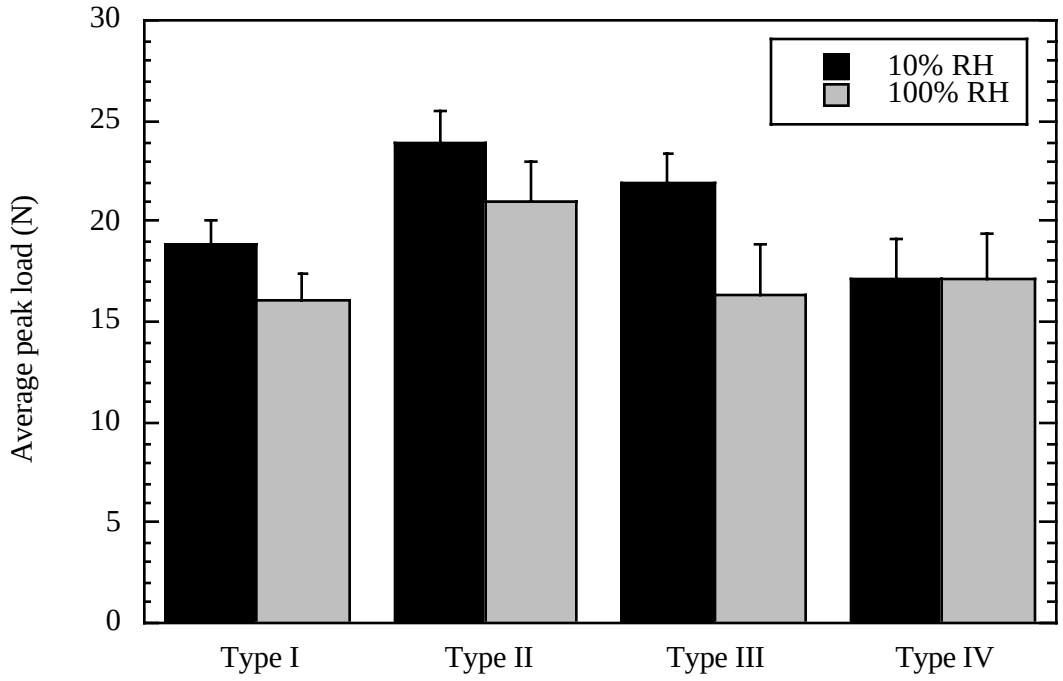

Fig. 3.9. Comparison of average peak load for each surface treatment at 10% and 100% RH levels.

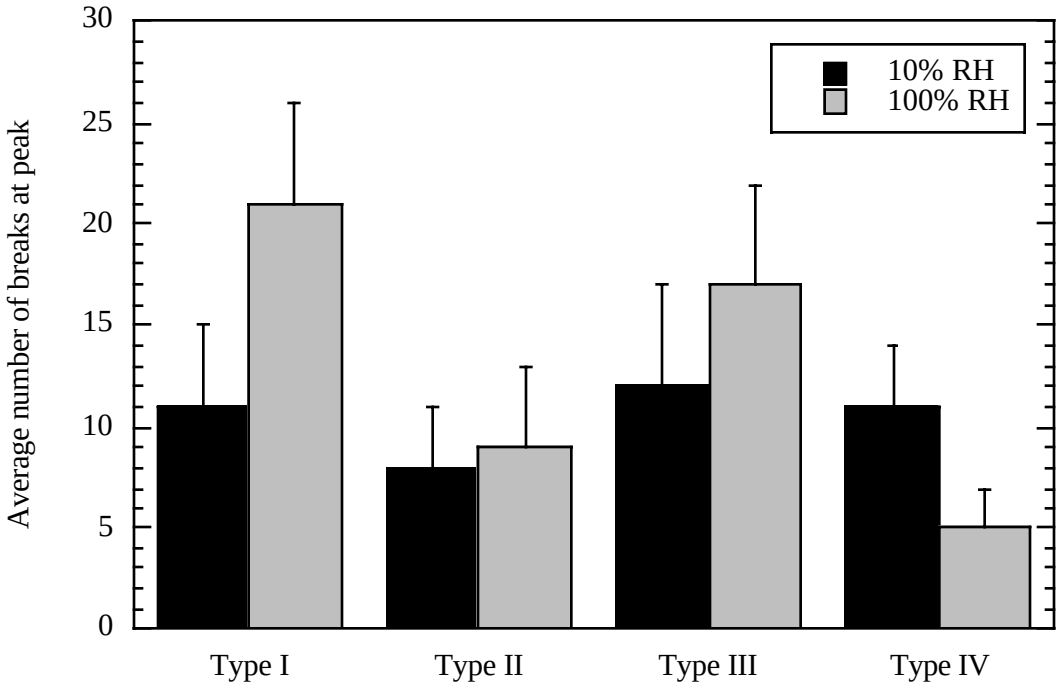

Fig. 3.10. Comparison of average number of breaks at peak load for each surface treatment at 10% and 100% RH.

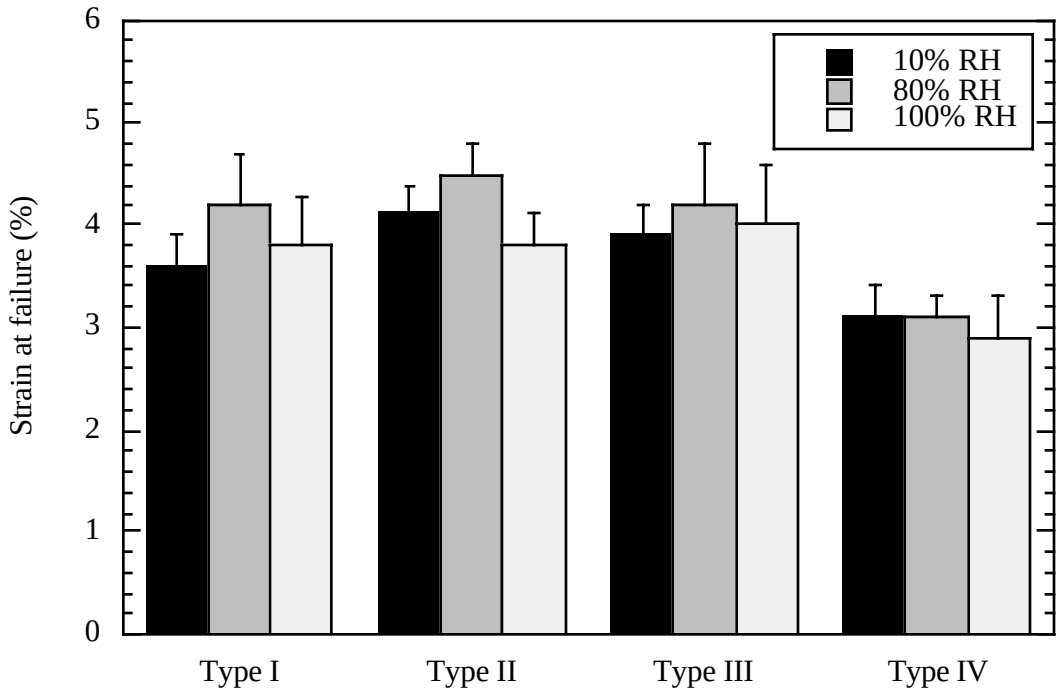

Fig. 3.11. Comparison of average strain to failure for each surface treatment at 10% and 100% RH.

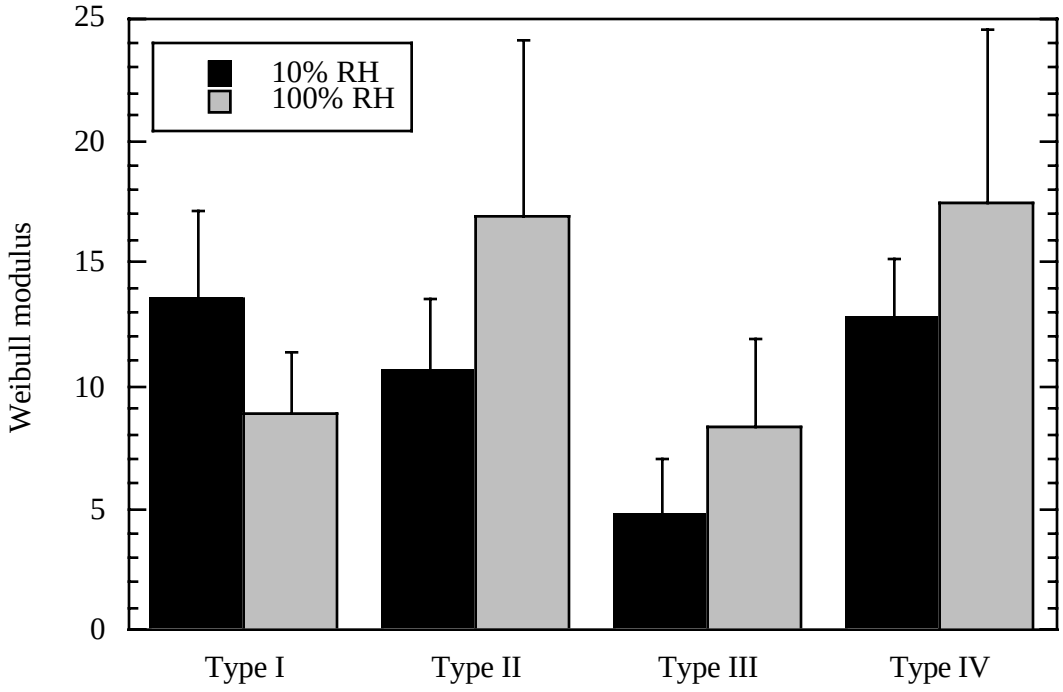

Fig. 3.12. Comparison of the average Weibull modulus for each surface treatment at 10% and 100% RH.

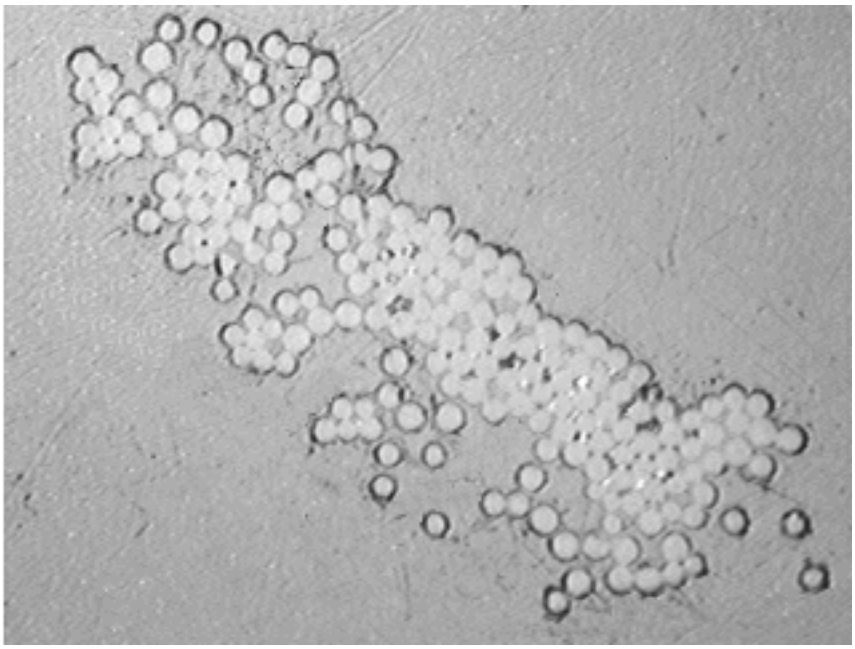

Fig. 3.13. Typical cross-section of a glass fiber bundle.

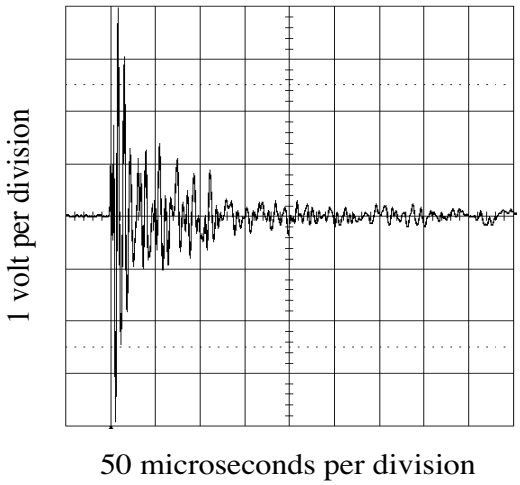

Fig. 3.14. Typical waveform for type I bundles conditioned at 40% RH.

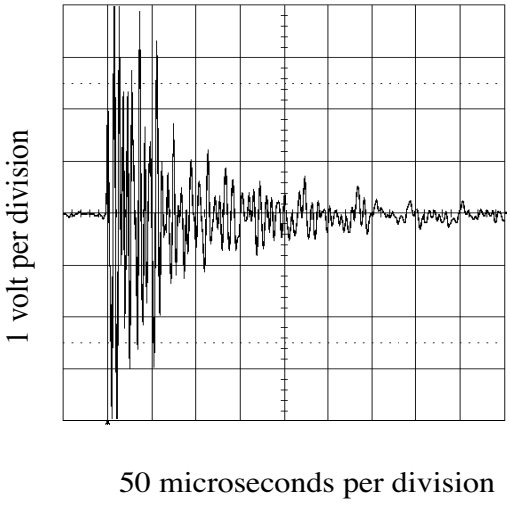

Fig. 3.15. Typical waveform for type II bundles conditioned at 40% RH.

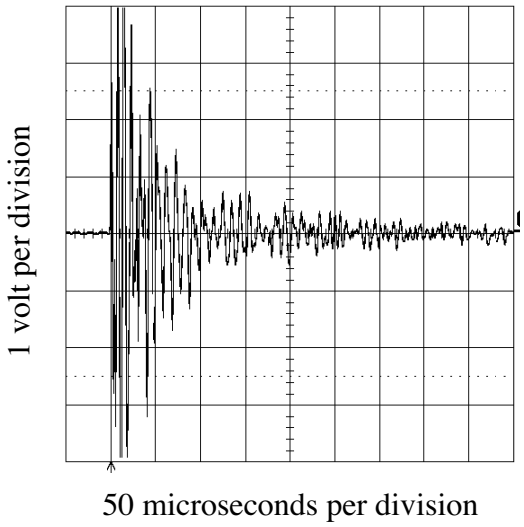

Fig. 3.16. Typical waveform for type III bundles conditioned at 40%RH.

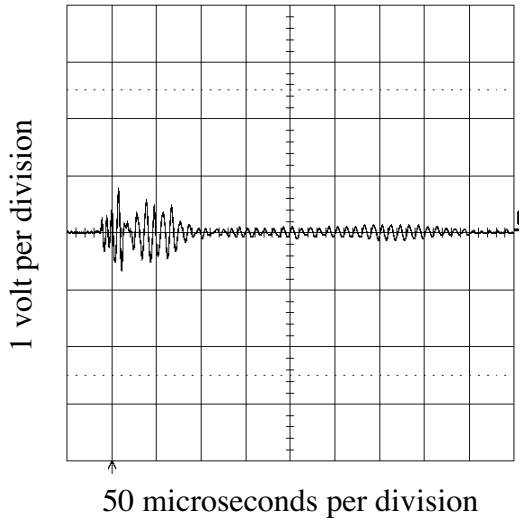

Fig. 3.17. Signal recorded during tension test of type III bundle conditioned at 40% RH.

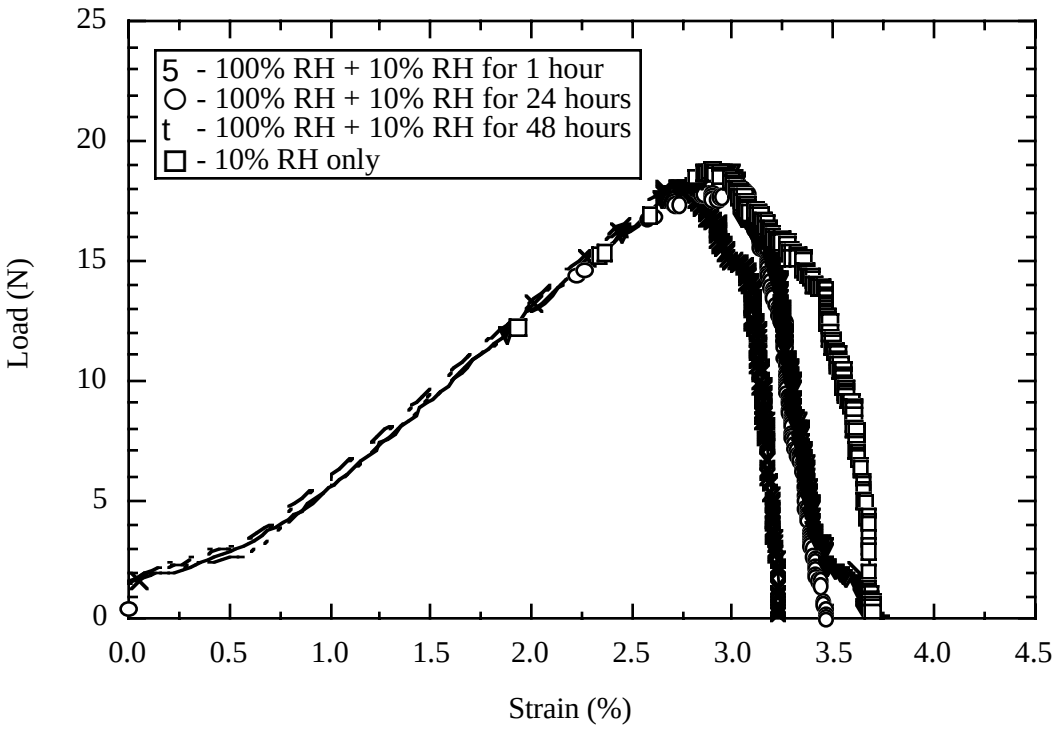

Fig. 3.20. Representative load–strain data for type I bundles conditioned at 10% RH only and at 100% RH for 24 hours followed by 10% RH for 1, 24 and 48 hours intervals.

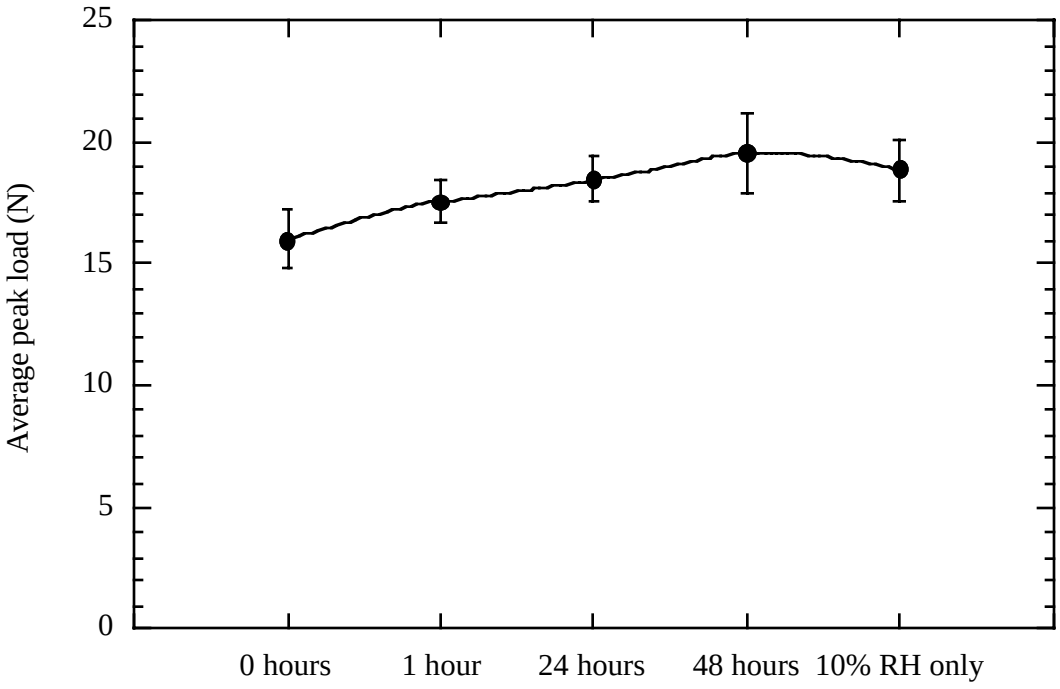

Fig. 3.21. Comparison of average peak loads for type I bundles conditioned at 100% RH then 0, 1, 24, and 48 hours at 10% RH and 10% RH only.

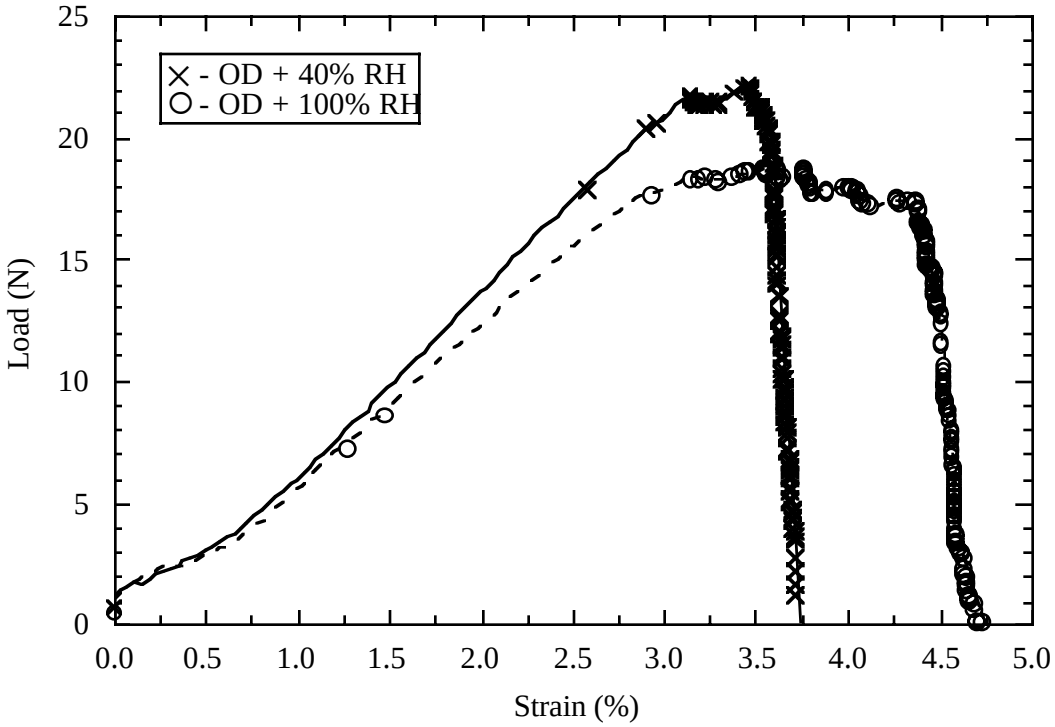

Fig. 3.22. Representative load–strain plot for OD + 40% and OD + 100% type II bundles.

Chapter 4

Effects of Twist

4.1 Introduction

Jones et al. (1971) showed that twisting a glass fiber bundle changes the tensile failure process and resultant strength characteristics. For an idealized twisted fiber bundle, the filaments lie along a helical path. The helix angle, θ, between the tangent to a helix and the bundle axis is a function of the fiber radius starting with zero at the center and reaching a maximum, θ_m, at the outer surface. The helix angle is related to the number of turns per unit length by

$$\tan\theta_m = 2\pi R_b T \tag{4.1}$$

where R_b is the bundle radius and T is amount of twist per unit length. Jones et al. (1971) assumed the change in strength was proportional to the helix angle. The effective modulus of a twisted bundle was reported by Zweben et al. (1979) to be lower than that of an untwisted yarn by a factor $\cos^2\theta_m$.

According to Zweben et al. (1979), twist causes radial stress in a loaded bundle. When a single fiber in a twisted bundle breaks, the separation of the broken ends is resisted by the friction between the fibers. The shear stresses acting on the surface of the fiber transfer load so that the effect of the break is localized. At some distance, Δ, from the break, the stress in a broken fiber is similar to that in an unbroken fiber. The distance Δ is the effective bundle length and the bundle can be considered to be a chain of bundles of length Δ. Gücer and Gurland (1962) developed a mathematical model for twisted fiber

strength, which is illustrated in Fig. 4.1. An estimate of the maximum stress at the center of the bundle is given by

$$\sigma_m^* = q(\theta_m)\sigma_f \tag{4.2}$$

where

$$q(\theta_m) = \frac{3}{4}\left(1 - \cos^2\theta_m\right) + \frac{1}{2}\ln(\cos\theta_m) \tag{4.3}$$

and σ_f is the fiber tensile stress, which is assumed to be constant throughout the bundle.

Zweben et al. (1979) compared experimental strength data from Kevlar fibers with predictions from the Gücer and Gurland (1962) model. The theory predicts a gradual increase in strength up to six turns per inch, then the strength will gradually decrease for for increasing twist. Zweben's experimental data show an increase in strength up to 2 turns per inch, then a dramatic decrease for increases in twist. A slightly different phenomenon was observed by Whitney (1966) for graphite fibers. A drop in strength was not detected until the twist exceeded 7 turns per inch.

Almost all glass fiber bundles are twisted to aid in winding. In this chapter, the effect of different levels of twist is presented for type I samples. All tests were performed with type I bundles conditioned at 40% RH. The data set used for zero turns/inch were taken from the type I, 40% RH data discussed in Chapter 3. The averages and standard deviations of all the twist data sets are summarized in Table 4.1.

Table 4.1. Averages and standard deviations of tensile data for type I bundles conditioned at 40% RH and twisted 0, 1, 2, 3 and 5 turns/inch.

Turns/inch	0	1	2	3	5
Peak load (N)	18.1 ± 2.1	18.6 ± 1.9	16.8 ± 1.2	17.8 ± 1.0	17.0 ± 1.8
Number of breaks at peak	13 ± 5	15 ± 6	19 ± 5	14 ± 5	25 ± 9
Strain at failure (%)	3.2 ± 0.3	3.4 ± 0.3	3.5 ± 0.4	3.6 ± 0.3	3.1 ± 0.2
Weibull modulus	6.6 ± 1.6	7.9 ± 2.1	8.5 ± 1.8	6.3 ± 0.9	6.1 ± 1.3

4.2 Experimental results

Typical load–strain plots for each level of twist are shown in Fig. 4.2. All levels of twist have a similarly shaped curve. Figure 4.3 compares the average peak load as the number of turns/inch increases. Overall, a gradual decrease in the peak load is observed with increasing twist. However, a slight increase in strength was observed at 1 and 3 turns/inch. In addition, the stress of twisting 5 turns/inch broke some of the weak filaments prior to the tensile test. As the number of turns/inch increases, the misalignment of the fibers with the loading direction causes a decrease in peak tensile load. As discussed in Section 4.1, a point of twist may be reached such that an apparent increase in strength can occur. At this point, the fibers support more load, such as in a rope, when wound together. However, the small 3% increase in peak load measured for bundles twisted 1 turn/inch was within the standard deviation of the average peak load. Therefore, no significant increase in tensile strength was observed at low levels of twist, as reported by Zweben et al. (1979) with Kevlar fibers.

A small increase in the strain to failure occurs between 0 and 3 turns/inch. At 5 turns/inch, the strain to failure decreases. Although no significant increase in strength occurred at low levels of twist, the strain to failure did increase. The inter-fiber load

transfer is one possible reason for the increase in strain to failure. Unfortunately, no comparison can be made because the previous work with twisted bundles did not cite the strain to failure. The average number of breaks at the peak is summarized in Fig. 4.4 for each level of twist. The number of breaks at peak increases with increasing twist, except at 3 turns/inch. At 5 turns/inch, the fibers began to break prior to the beginning of the test. This result correlates with the very large number of breaks at peak load for that level of twist.

The average Weibull modulus for each level of twist is shown in Fig. 4.5. A slight increase is noticed for 1 and 2 turns/inch. For larger amounts of twist (3 and 5 turns/inch), the Weibull modulus is within the standard deviation of the average Weibull modulus for bundles with no twist. The Weibull modulus for bundles with lower levels of twist may increase due to the inter-fiber load transfer.

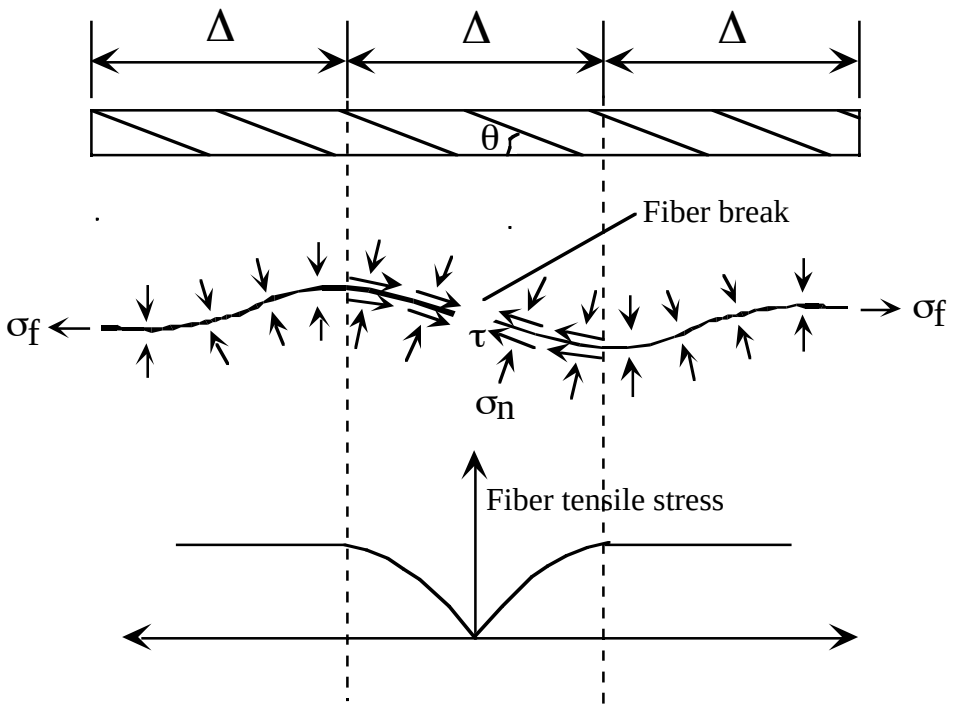

Fig. 4.1. Model for the tensile strength of twisted yarn.

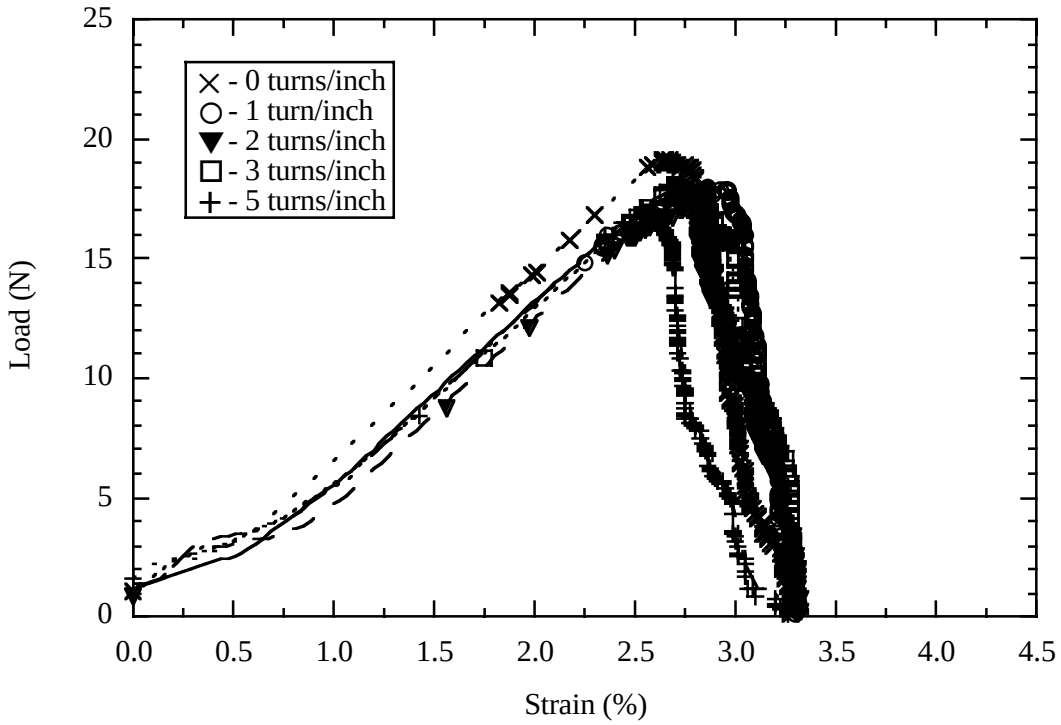

Fig. 4.2. Representative load–strain plot for type I at all levels of twist.

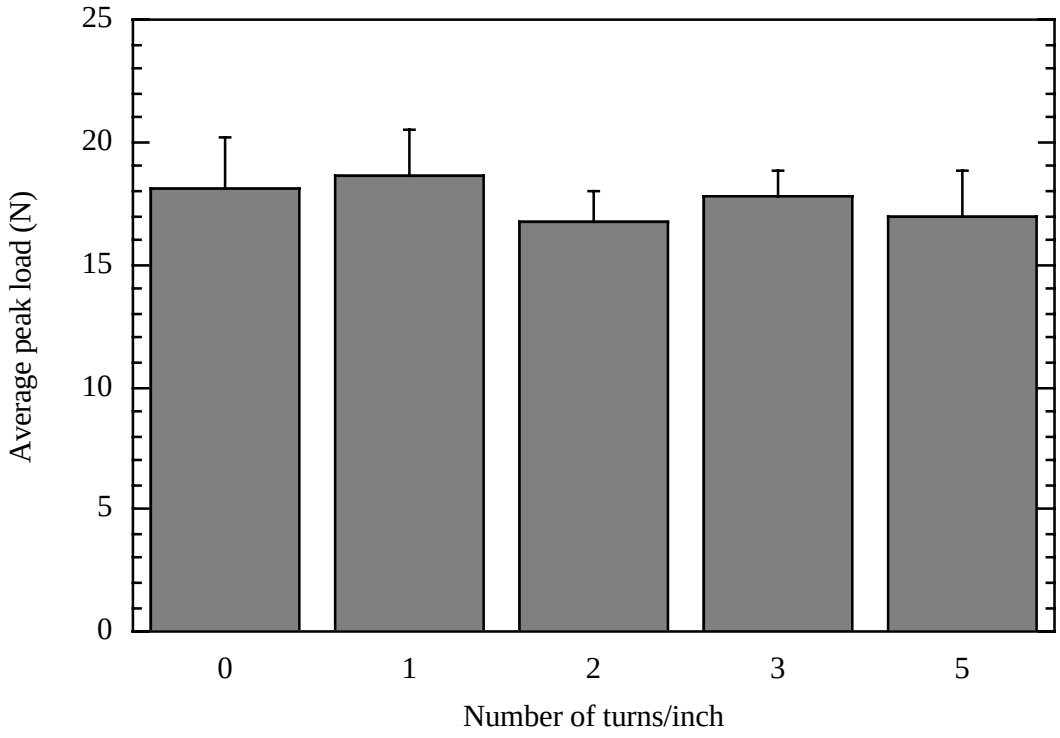

Fig. 4.3. Comparison of average peak load for each increase in the number of turns/inch.

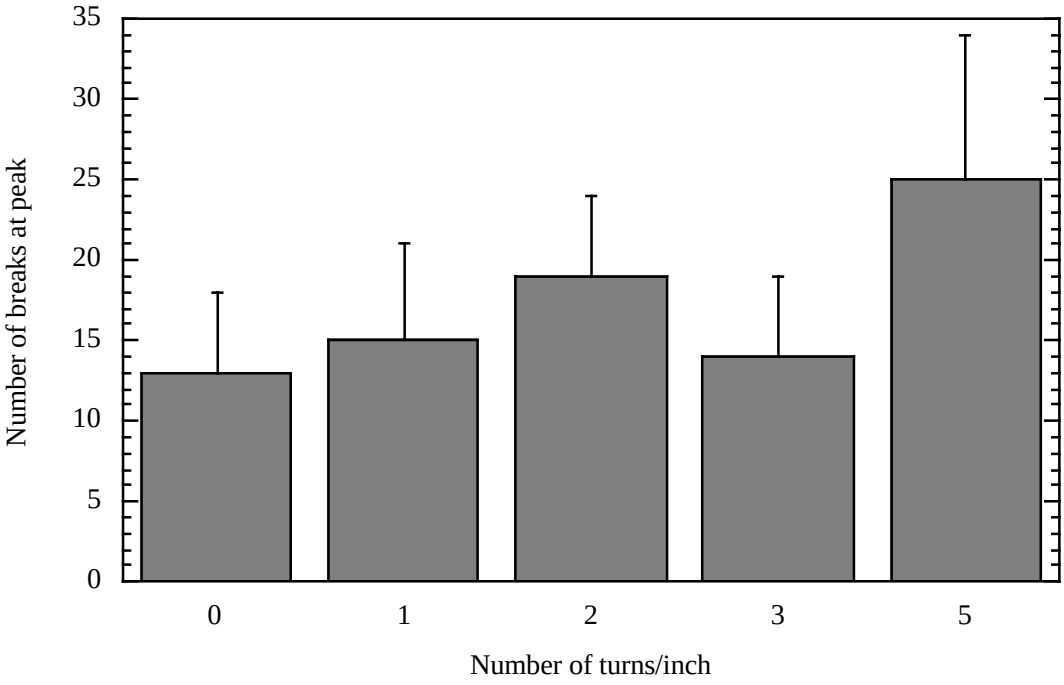

Fig. 4.4. Comparison of number of breaks at peak load for each increase in the number of turns/inch.

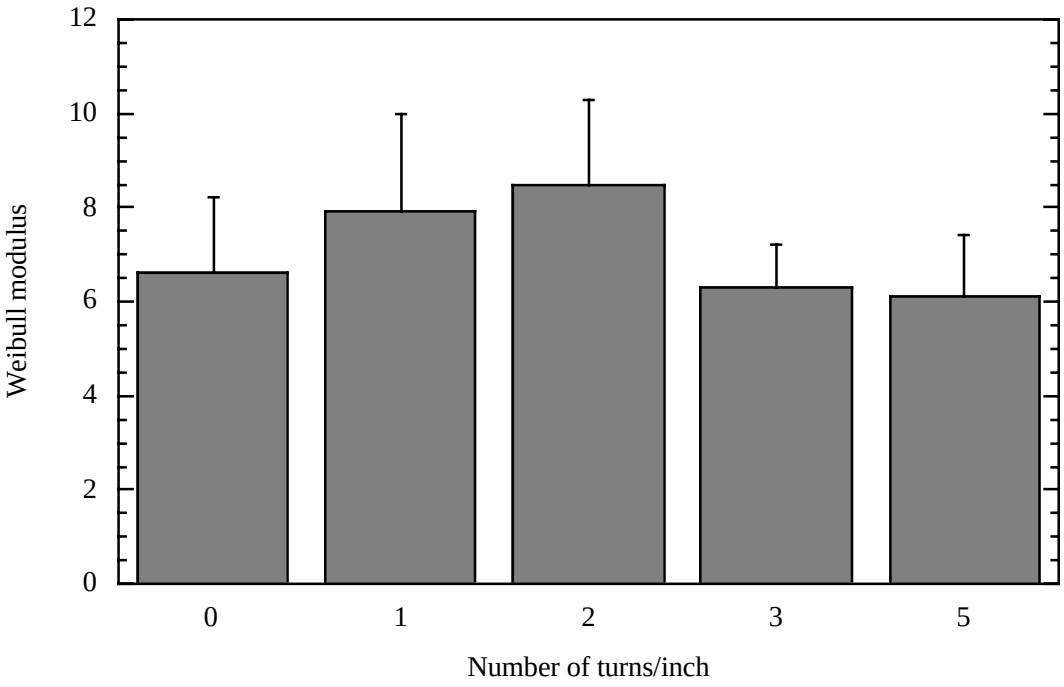

Fig. 4.5. Comparison of the Weibull modulus for each increase in number of turns/inch.

Chapter 5

Conclusions

A comprehensive test program was completed for four types of surface treatment at four different levels of humidity. A moisture reversibility study was completed for type I bundles, and the influence of oven-drying was investigated for type II fibers. In addition, five different levels of twist were tested using type I fibers at 40% RH. Samples with a one-inch gage length were tested in tension using an AE sensor to detect each fiber break. An oscilloscope recorded the peak load and time for each fiber break in the bundle. The load–displacement data from the Instron and the load–time data from the AE sensor were used to create load–strain plots from which the peak load, number of breaks at the peak, and strain to failure were recorded for each test. From the AE data, Weibull plots were made and the Weibull modulus was calculated for each test. Averages and standard deviations from each data set were compared with each other.

Four types of surface treatment were included in this study: starch (type I), starch and silane (type II), starch and wax (type III), and epoxy (type IV). Fiber bundles with each surface treatment were tested at 10%, 40%, 80% and 100% RH. The starch/silane surface treatment had the highest peak load at each humidity level, even with a drop in average peak load at 100% RH. At 10%, 40% and 80% RH, the starch and wax surface treatment had a higher peak load than types I and IV; however, at 100% RH the type III fibers had a large decrease in average peak load. The type IV fibers had a low average peak load that was consistent at all levels of humidity.

The tensile strength of the glass fiber bundles is highly dependent on the amount of surface damage due to moisture absorption and contact abrasion. The different surface treatments considered in this investigation appear to alter the amount of damage from both these effects. A considerable increase in the average peak load was measured for the type II bundles at all levels of humidity. The silane added to the starch chemistry in type II samples prevents moisture absorption throughout the life of the fibers. High tensile strength values were also measured for type II bundles at low humidity levels. The wax additive in type III bundles serves as a lubricant that protects the fibers from surface damage. The average peak load for the wax treated fibers decreased dramatically when soaked at 100% RH. Although the wax effectively prevents surface damage at low humidity, it does not protect against moisture damage at high humidity levels. Type IV bundles had the lowest average peak load at each humidity level. Type IV bundles have an epoxy size with a very different chemistry than types I, II, and III samples. The epoxy size may have increased the surface roughness and caused a decrease in tensile strength due to increased contact abrasion.

Type II bundles were tested at 40% and 100% RH after oven-drying to ensure a full cure of the silane. At both 40% and 100% RH, no difference was measured between the average peak loads for the oven-dried and the not oven-dried bundles. However, at 100% RH the number of breaks at peak load and strain to failure for the oven-dried bundles were much larger than the not oven-dried.

A reversibility study was completed by soaking type I bundles for 24 hours and then drying out the bundles at 10% RH for 1, 24, or 48 hours. A steady increase in average peak load was shown for each increase in the time at 10% RH. The average peak load for the bundles at 10% RH for 48 hours was similar to the average peak load for bundles placed only in the 10% RH environment. These results imply that short-term water damage is reversible.

Type I bundles were twisted to 0, 1, 2, 3, and 5 turns/inch and tested at 40% RH. A large change in average peak load was not observed for any level of twist tested. The highest average peak load was at 1 turn/inch, but the average peak load for 0 turns/inch was similar. The lowest peak load was at 2 turns/inch, which was followed by an increase for 3 turns/inch and then a decrease at 5 turns/inch.

5.1 Future work

For this study, the fiber bundles were kept in the humidity environment for at least 24 hours before testing, but the test was run at room humidity (approximately 40% RH). The duration of the test was not longer than one-half hour, and it was assumed that a significant change in strength would not occur in that time period. To ensure accuracy, bundles could be tested in the conditioned environment.

The most probable reason for the higher strength of the silane treated fibers was that the fibers were protected from moisture damage over the entire life of the fiber. If moisture damage is the key factor, then other types of bundles should be able to reach

higher peak loads if stored in a low humidity environment directly after manufacture. Testing types I, III, and IV at 10% RH directly after manufacturing would provide a definite conclusion.

Fiber bundle strength is highly influenced by the amount of contact abrasion between the fibers. The roughness of the fiber surface determines the amount of abrasion. Measuring the surface roughness of the different types of fiber bundles could show a direct correlation between strength and contact abrasion.

Appendix

Individual Bundle Data

A.1. Table of tensile data for type I bundles conditioned at 10% RH.

Sample	Peak load (N)	Breaks at peak	Strain to failure (%)	Weibull modulus	Total breaks
1	20.8	9	3.70	18.3	166
2	20.8	7	3.70	14.1	170
3	16.8	10	3.70	13.5	203
4	19.2	13	3.11	14.6	189
5	18.1	12	3.43	13.5	186
6	19.9	10	3.66	13.8	177
7	19.4	9	3.43	10.6	202
8	19.7	10	3.62	10.1	178
9	17.5	21	4.17	8.1	200
10	17.4	12	3.66	17.6	200
11	17.5	12	3.11	12	198
12	18.3	13	3.31	14.3	189
13	19.8	6	3.27	14.8	191
14	17.6	17	3.82	9.5	184
15	17.9	6	3.15	13.3	191
16	19.8	11	3.82	11.7	190
17	18.7	9	3.70	9.3	180
18	20.5	11	3.58	22.9	171
19	18.7	9	4.21	13.3	187
20	19.6	8	3.78	16.7	176
Average	18.9	11	3.6	13.6	186
Standard deviation	1.2	4	0.3	3.5	11

A.2. Table of tensile data for type I bundles conditioned at 40% RH.

Sample	Peak load (N)	Breaks at peak	Strain at failure (%)	Weibull modulus	Total breaks
1	17.0	5	2.72	7.46	193
2	19.4	3	3.11	7.96	195
3	16.7	9	2.83	4.4	192
4	20.3	22	3.54	5.75	187
5	18.9	8	3.31	6.07	178
6	19.9	16	3.35	4.31	190
7	16.4	13	3.66	6.72	192
8	19.6	19	3.35	6.03	188
9	16.7	8	2.80	8.71	201
10	16.0	21	2.95	5.67	194
11	16.2	5	2.83	8.83	196
12	16.3	14	2.99	6.03	189
13	16.1	14	2.68	5.34	194
14	16.6	11	2.83	7.5	193
15	15.8	15	2.64	4.87	199
16	23.1	10	3.82	7	162
17	17.4	17	3.70	8.3	178
18	17.3	20	3.50	10.2	185
19	20.2	9	3.27	6.2	167
20	19.9	13	3.35	7.7	188
21	18.1	12	3.31	5.22	187
22	18.5	8	3.35	8.23	180
23	15.9	11	2.99	7.71	195
24	16.8	20	3.23	4.71	190
25	18.3	21	3.35	4.58	196
26	22.5	13	3.46	5.95	188
Average	18.1	13	3.2	6.6	188
Standard deviation	2.0	5	0.3	1.6	9

A.3. Table of tensile data for type I bundles conditioned at 80% RH.

Sample	Peak load (N)	Breaks at peak	Strain at failure (%)	Weibull modulus	Total breaks
1	19	16	3.78	13.7	168
2	15.1	25	4.84	3.9	170
3	18.2	21	4.92	6.9	165
4	22.3	5	3.90	4.8	163
5	19.7	24	3.94	6.1	169
6	20.1	13	3.98	8.2	169
7	19.5	6	4.72	11.3	176
8	15.2	16	5.12	10.5	167
9	19.1	21	4.25	6.8	179
10	17.2	9	3.50	11.5	177
11	20.8	18	4.13	7.4	160
12	20.4	7	3.54	11.5	159
13	16.5	12	3.50	5.6	177
14	17.8	6	3.50	12.5	160
15	20.3	14	5.04	6.3	159
16	19.5	11	4.33	7.1	177
17	18.3	19	3.86	4.8	188
18	15.6	22	4.72	12	176
19	19.2	18	4.53	7.4	161
20	17.8	10	3.86	11.2	169
Average	18.6	15	4.2	8.5	170
Standard deviation	1.9	6	0.5	3.0	8

A.4. Table of tensile data for type I bundles conditioned at 100% RH.

Sample	Peak load (N)	Breaks at peak	Strain to failure (%)	Weibull modulus	Total breaks
1	16.4	19	3.94	8.6	189
2	15.8	26	3.78	7.4	192
3	14.8	27	3.39	7.6	167
4	15.1	18	3.86	6.2	188
5	14.1	25	3.39	7.1	197
6	15.3	18	4.33	12.4	181
7	15.3	28	3.74	9.9	188
8	17.4	21	3.82	8.6	189
9	16	15	3.74	6.2	191
10	15.8	23	3.50	9.3	183
11	16.2	20	3.74	12.0	186
12	18.4	22	3.86	13.9	184
13	18.5	21	3.35	14.2	169
14	15.9	12	4.65	7.6	175
15	17.3	16	3.54	8.1	190
16	16.3	21	3.19	7.4	186
17	14.9	28	4.33	5.9	171
18	15.1	20	3.50	7.1	189
Average	16.0	21	3.8	8.9	184
Standard deviation	1.2	5	0.4	2.6	8

A.5. Table of tensile data for type II bundles conditioned at 10% RH.

Sample	Peak load (N)	Breaks at peak	Strain to failure (%)	Weibull modulus	Total breaks
1	25.6	16	4.21	8.7	133
2	26	3	4.17	15.7	146
3	25.8	5	4.13	10.2	152
4	23.9	7	3.70	9.5	142
5	22.8	6	5.00	6.3	194
6	23.7	7	3.82	13.9	155
7	22.9	6	3.82	15.5	160
8	24	8	3.94	9.5	175
9	24.3	9	4.41	7.8	169
10	22.4	6	4.25	5.9	170
11	23.2	7	3.58	13.3	174
12	20	8	4.02	10.9	171
13	24.6	14	4.65	7	161
14	23.7	8	4.06	9	155
15	24	7	4.21	7.4	152
16	23	10	3.78	14.5	155
17	23.1	9	4.53	10.6	172
18	24.2	12	4.06	9.7	128
19	25.5	8	4.13	15.2	171
20	26.2	9	4.33	10.5	182
Average	23.9	8	4.1	10.6	161
Standard deviation	1.5	3	0.3	3.1	16

A.6. Table of tensile data for type II bundles conditioned at 40% RH.

Sample	Peak load (N)	Breaks at peak	Strain to failure (%)	Weibull modulus	Total breaks
1	23.8	9	3.82	6	184
2	23.9	18	3.82	7.06	174
3	24.1	11	3.86	7.2	185
4	21.4	5	3.03	7.26	192
5	19.2	15	3.50	3.62	175
6	22	5	3.74	6.53	179
7	23.3	9	3.46	5.96	157
8	20.8	5	3.07	9.91	197
9	21.8	6	3.43	8.78	174
10	21.6	6	3.19	8.92	202
11	16.9	8	2.87	4.45	191
12	22.8	6	3.43	7.74	194
13	21.9	5	3.19	7.45	203
14	24.6	4	3.54	8.06	167
15	25	14	3.98	5.93	186
16	24.9	3	3.70	8.72	170
17	23.4	4	3.74	8.33	128
18	23.1	6	3.66	7.98	163
19	22.6	9	3.46	6.75	190
20	27.7	13	3.86	5.56	91
Average	22.7	8	3.5	7.1	175
Standard devation	2.3	4	0.3	1.6	26

A.7. Table of tensile data for type II bundles conditioned at 80% RH.

Sample	Peak load (N)	Breaks at Peak	Strain to failure (%)	Weibull modulus	Total breaks
1	21.3	4	3.94	7.08	140
2	25.5	6	4.53	20.8	123
3	26.5	5	4.96	26.1	106
4	24.1	7	4.45	16.1	103
5	25.4	11	4.61	14.5	99
6	24.2	10	4.53	5.6	140
7	23	3	4.80	9.5	148
8	24.7	9	4.61	17.2	135
9	23.3	4	4.06	11.5	145
10	24.3	9	4.45	16.9	116
11	25.8	11	4.61	20.6	94
12	22.8	13	4.25	9.1	139
13	24.1	11	4.65	26.8	130
14	22.7	18	4.41	10.8	149
15	24.7	10	4.72	15.6	125
16	25.5	10	4.65	18.2	140
17	24.6	11	4.57	6.9	155
18	23.1	5	4.76	10.5	162
19	25.5	15	3.86	22	170
20	26	6	4.53	10.5	121
Average	24.4	9	4.5	14.8	132
Standard deviation	1.3	4	0.3	6.3	21

A.8. Table of tensile data for type II bundles conditioned at 100% RH.

Sample	Peak load (N)	Breaks at peak	Strain to failure (%)	Weibull modulus	Total breaks
1	22	8	3.94	4.59	179
2	21.3	7	3.50	30.3	174
3	23.3	14	4.33	11.37	184
4	21.3	11	3.94	13.7	189
5	22.1	8	3.86	16.5	176
6	21.9	7	3.43	13.8	165
7	19.6	12	3.39	9.7	168
8	17.3	13	3.82	8.62	189
9	21.6	10	3.98	7.58	161
10	23	6	3.74	28.6	161
11	19.1	12	3.74	23.1	158
12	20.6	4	3.98	19.9	174
13	21.4	5	4.06	21.3	192
14	19.9	9	3.39	16.8	198
15	21.2	12	3.31	22	165
16	18.3	15	4.45	13.3	172
17	22	4	3.46	24	171
18	20.6	5	3.82	18.56	179
Average	21.0	9	3.8	16.9	175
Standard deviation	1.6	4	0.3	7.2	12

A.9. Table of tensile data for type III bundles conditioned at 10% RH.

Sample	Peak load (N)	Breaks at peak	Strain to failure (%)	Weibull modulus	Total breaks
1	18.9	27	3.19	3.8	186
2	23.3	7	3.58	7.1	173
3	21.6	13	3.35	2.3	175
4	20.1	20	3.82	3.1	190
5	21.2	11	4.06	2.2	189
6	20	13	3.86	10.3	138
7	23.5	15	4.69	4.2	200
8	24	7	3.98	2.2	138
9	22.5	6	3.98	2.3	147
10	22.4	16	4.17	6.6	168
11	22.3	10	4.17	3.3	200
12	21.9	10	3.78	9.4	157
13	22.6	11	3.94	5.8	164
14	21.3	8	3.98	2.2	152
15	22.9	5	3.86	6.1	151
16	22.3	11	3.86	6.2	158
17	21.5	8	3.94	3.5	167
18	23.8	12	4.33	4.6	142
19	22.5	10	3.86	2.5	156
20	22.6	11	4.06	6.2	148
Average	22.1	12	3.9	4.7	165
Standard deviation	1.3	5	0.3	2.4	20

A.10. Table of tensile data for type III bundles conditioned at 40% RH.

Sample	Peak load (N)	Breaks at peak	Strain to failure (%)	Weibull modulus	Total breaks
1	21.2	19	3.50	3.2	183
2	23	5	4.09	5.5	163
3	22.3	11	3.46	3.2	174
4	21.8	21	4.41	2.7	185
5	23.5	4	3.62	5.5	160
6	20.1	21	3.50	3.1	183
7	23.1	11	3.35	6.4	153
8	17.9	36	3.50	3.7	187
9	22.8	22	3.46	2.6	182
10	20.2	22	3.82	2.8	186
11	21.7	10	3.39	4.0	173
12	20.3	27	3.90	2.7	204
13	20.7	17	3.54	2.8	183
14	19.7	9	3.11	4.3	176
15	20.6	21	3.78	2.3	187
16	22.6	21	4.02	2.5	180
17	20.8	25	3.78	3.5	185
18	21.2	16	3.98	2.9	176
19	19.7	26	3.62	5.4	189
20	21.1	11	3.62	6.8	185
Average	20.7	20	3.7	3.6	184
Standard deviation	1.3	8	0.3	1.3	8

A.11. Table of tensile data for type III bundles conditioned at 80% RH.

Sample	Peak load (N)	Breaks at peak	Strain to failure (%)	Weibull modulus	Total breaks
1	20.9	11	4.80	5.5	172
2	25.3	9	4.33	6.6	185
3	23.9	10	4.13	4.4	98
4	23.9	7	3.94	5.3	110
5	22.1	32	3.50	4	121
6	20.7	22	3.62	2.9	162
7	22.2	13	4.37	6.8	127
8	20.8	14	5.47	2.2	192
9	17.6	17	3.94	8.2	156
10	20.1	15	3.86	6.3	159
11	19.8	15	3.70	5.9	162
12	20.9	14	4.33	12	163
13	21.1	11	5.31	7.1	130
14	23.4	10	5.04	3.5	191
15	24.6	8	4.13	7.5	152
16	23.8	16	3.90	7.6	163
17	26.2	15	3.82	6.2	158
18	21.3	20	3.54	3.2	162
19	21.9	27	4.02	4.5	126
20	18.9	6	4.09	5.6	113
Average	22.0	14	4.2	5.8	150
Standard deviation	2.2	6	0.6	2.2	27

A.12. Table of tensile test data for type III conditioned at 100% RH.

Sample	Peak load (N)	Breaks at peak	Strain to failure (%)	Weibull modulus	Total breaks
1	11.8	17	5.16	3.31	170
2	17.6	24	4.41	7.36	168
3	16.1	23	3.98	5.6	162
4	17.1	20	4.33	4.64	180
5	16	17	4.80	5.92	142
6	17.9	21	4.33	10.5	182
7	18.2	11	3.58	15.4	172
8	14.3	18	3.98	8.8	186
9	16.5	22	3.86	5.4	178
10	15.8	15	3.78	7.2	164
11	17.2	19	4.72	9.5	167
12	18	21	3.82	10.2	182
13	16.2	25	3.70	8.6	185
14	16.4	16	4.09	6.5	174
15	16.8	10	3.39	11.6	153
16	15.9	12	3.39	7.5	149
17	13.5	21	3.19	9.21	154
18	18.1	15	3.54	17.6	167
19	20.5	8	3.39	7.46	180
20	13.7	12	3.50	3.91	123
Average	16.4	17	3.9	8.3	167
Standard deviation	2.0	5	0.5	3.6	16

A.13. Table of tensile data for type IV bundles conditioned at 10% RH.

Sample	Peak load (N)	Breaks at Peak	Strain to failure (%)	Weibull modulus	Total breaks
1	16.1	14	2.91	6.81	204
2	15.7	9	3.07	13.8	194
3	17.2	14	3.07	13.7	192
4	17.8	11	3.15	14.3	192
5	15.8	14	2.83	12.4	198
6	16.9	7	3.11	16.3	191
7	23	5	3.78	12	167
8	18.2	10	3.07	15.5	187
9	16	12	2.95	14	179
10	21.3	13	3.74	10.7	168
11	15.7	7	2.72	9.9	193
12	20.1	13	3.66	12.7	176
13	16.2	10	3.07	12	196
14	15.6	10	2.99	13.8	196
15	13.9	10	2.95	9.7	198
16	16.4	10	3.03	12.7	198
17	16.8	9	3.11	16.5	176
18	17.1	12	3.15	13.1	188
19	15.9	13	2.99	12.1	179
20	16.5	7	3.07	13.6	190
Average	17.1	11	3.1	12.8	188
Standard deviation	2.1	3	0.3	2.3	11

A.14. Table of tensile data for type IV bundles conditioned at 40% RH.

Sample	Peak load (N)	Breaks at peak	Strain to failure (%)	Weibull modulus	Total breaks
1	18.1	10	3.07	5.0	188
2	19	10	3.19	6.2	189
3	14.9	6	2.72	15.6	195
4	20.2	4	3.23	9.4	190
5	19.3	13	3.07	5.2	193
6	15.9	8	2.95	12.8	198
7	16.9	9	2.83	6.5	192
8	18.2	5	2.99	6.6	191
9	25.3	4	3.58	10.0	144
10	20.1	9	3.31	7.4	171
11	15.3	4	2.72	15.3	195
12	17.4	10	2.91	18.2	188
13	15.5	7	2.56	21.1	193
14	21.1	8	3.58	16.1	169
15	21.9	3	3.46	14.4	182
16	23.5	3	2.68	20.4	165
17	15.9	7	2.76	18.1	198
18	15	9	2.80	14.5	193
19	15.7	7	3.07	16.5	194
20	14.6	10	2.99	5.8	198
Average	18.4	7	3.0	14.2	183
Standard deviation	3.6	3	0.3	5.2	16

A.15. Table of tensile data for type IV bundles conditioned at 80% RH.

Sample	Peak load (N)	Breaks at peak	Strain at failure (%)	Weibull modulus	Total breaks
1	15.1	10	2.76	12.4	189
2	14.9	4	2.87	13.8	200
3	15.8	9	3.11	14.4	195
4	18.6	15	3.11	16.1	194
5	16.9	14	3.19	12.1	196
6	14.7	4	3.15	14.3	185
7	19	6	2.91	23.4	187
8	17.3	13	3.23	21.9	189
9	16.4	11	3.19	12.2	185
10	17.2	12	3.15	14.1	186
11	15.8	12	3.15	12.8	195
12	17.2	10	2.95	14.6	190
13	14.7	14	3.23	5.8	192
14	15.9	10	3.23	15.1	186
15	17.5	14	3.19	14.2	189
16	15.8	7	3.27	13.5	188
17	17.2	6	3.15	12.5	186
18	17.9	12	2.99	11.6	195
19	16.1	16	3.11	16.8	194
20	15.2	8	3.27	12.3	182
Average	16.5	10	3.1	14.2	190
Standard deviation	1.3	4	0.1	3.7	5

A.16. Table of tensile data for type IV bundles conditioned at 100% RH.

Sample	Peak load (N)	Breaks at peak	Strain to failure (%)	Weibull modulus	Total breaks
1	16.5	6	2.72	8.4	195
2	20.3	3	3.07	26.9	187
3	16.8	10	2.68	18.2	172
4	17.4	4	2.83	8.1	183
5	18.1	3	2.99	18.8	191
6	16.9	8	2.91	9.5	185
7	16.8	9	3.15	16.2	179
8	18.2	5	2.68	24.5	194
9	15.9	4	3.03	26	192
10	14.5	3	2.64	18.6	179
11	20.6	5	3.03	7.4	172
12	15.4	4	2.68	21.5	193
13	17	8	3.03	23.9	167
14	19	4	3.78	26.5	169
15	20.1	4	2.95	7.6	183
16	16	6	2.83	16.9	204
17	16.5	5	3.23	25.6	182
18	15.4	5	2.80	18.7	180
19	14.9	5	2.40	7.4	151
20	16.4	7	2.91	17.1	147
Average	17.1	5	2.9	17.4	180
Standard deviation	1.8	2	0.3	7.1	14

A.17. Table of tensile data for type I bundles conditioned at 100% RH, then 10% RH for 1 hour.

Sample	Peak load (N)	Breaks at peak	Strain to failure (%)	Weibull modulus	Total breaks
1	16.8	12	3.11	10.6	189
2	18.4	16	3.62	9.6	181
3	17.0	10	3.07	11.8	193
4	19.0	11	3.35	12.4	190
5	16.8	6	3.11	14.3	192
6	17.8	5	3.23	12.9	183
Average	17.6	10	3.2	11.9	188
Standard deviation	0.9	4	0.2	1.7	5

A.18. Table of tensile data for type I bundles conditioned at 100% RH, then 10% RH for 24 hours.

Sample	Peak load (N)	Breaks at peak	Strain to failure (%)	Weibull modulus	Total breaks
1	19.7	8	3.62	13.9	166
2	17.6	20	3.39	10.2	188
3	17.9	9	3.50	9.8	182
4	18.0	15	3.19	13.7	193
5	18.4	13	3.46	12.1	183
6	19.4	17	3.66	9.4	186
Average	18.5	14	3.5	11.5	183
Standard deviation	0.9	5	0.2	2.0	9

A.19. Table of tensile data for type I bundles conditioned at 100% RH, then 10% RH for 48 hours.

Sample	Peak load (N)	Breaks at Peak	Strain to failure (%)	Weibull modulus	Total breaks
1	17.2	9	3.27	14.3	194
2	19	14	3.66	13.2	187
3	20.6	13	3.31	14.6	192
4	21.4	16	3.94	8.5	170
5	19.8	12	3.74	9.6	183
Average	19.6	13	3.6	12.0	185
Standard deviation	1.6	3	0.3	2.8	10

A.20. Table of tensile data for type II bundles oven-dried, then conditioned at 40% RH.

Sample	Peak load (N)	Breaks at peak	Strain to failure (%)	Weibull modulus	Total breaks
1	19.7	17	3.19	6.2	168
2	25.9	3	3.94	12.2	119
3	21.1	15	3.66	13.2	185
4	25.7	7	4.21	16.5	115
5	21.2	5	3.54	18.4	182
6	22.2	2	4.09	15.6	164
7	25.1	10	3.58	10.5	149
8	21.1	18	5.12	10.3	195
9	22.0	3	3.78	11.4	158
10	24.0	7	3.82	9.3	147
11	22.4	6	3.70	10.9	160
12	21.5	15	3.86	15.9	163
13	25.8	5	3.98	14.3	117
Average	22.9	9	3.88	12.7	156
Standard deviation	2.1	6	0.45	3.4	26

A.21. Table of tensile data for type II bundles oven-dried, then conditioned at 100% RH.

Sample	Peak load (N)	Breaks at peak	Strain to failure (%)	Weibull modulus	Total breaks
1	16.1	26	3.07	4.1	203
2	18.8	25	4.72	9.6	171
3	16.3	23	4.53	5.9	193
4	17.1	24	4.65	6.1	187
5	16.3	25	5.16	5.7	203
6	21.9	15	3.70	18.1	183
7	17.5	22	4.57	5.1	188
8	15.9	24	4.76	6.2	202
9	22.1	18	3.74	17.6	186
10	17.5	20	4.41	7.5	179
11	20.2	18	4.53	15.4	191
12	16.4	22	4.84	6.9	197
13	17.9	23	4.65	7.3	200
Average	17.8	22	4.4	8.2	191
Standard deviation	2.2	3	0.6	5.2	10

A.22. Table of tensile data for type I bundles twisted 1turn/inch.

Sample	Peak load (N)	Breaks at peak	Strain to failure (%)	Weibull modulus	Total breaks
1	17.2	17	3.15	5.9	196
2	17.5	19	3.11	4.8	193
3	17.0	19	4.06	8.7	202
4	17.3	26	3.39	4.2	204
5	21.3	18	3.31	8.3	178
6	19.1	10	3.31	8.3	192
7	20.9	15	3.62	7.8	189
8	22.4	9	3.50	5.1	179
9	17.2	9	3.19	6	139
10	17.3	11	3.35	10.9	198
11	22.0	12	3.35	8.6	177
12	16.2	22	3.27	9	185
13	17.2	9	3.50	8.6	197
14	19.6	10	3.98	11.4	188
15	17.8	23	3.39	7.9	193
16	19.4	18	3.62	10.7	184
17	16.7	11	3.11	10.4	194
18	17.0	19	3.15	7.1	186
19	18.6	10	3.35	8.3	191
20	20.1	8	3.58	5.6	185
Average	18.6	15	3.4	7.9	188
Standard deviation	1.9	6	0.3	2.1	14

A.23. Table of tensile data for type I bundles twisted 2 turns/inch.

Sample	Peak load (N)	Breaks at peak	Strain to failure (%)	Weibull modulus	Total breaks
1	14.9	20	3.15	6.6	195
2	18.1	25	3.70	7.9	197
3	16	21	4.25	8.9	198
4	16.9	20	3.23	9.8	196
5	16.4	26	3.43	8	191
6	16.8	22	3.07	6.7	200
7	14.3	23	3.07	5.9	195
8	15.9	21	4.21	7	189
9	16.2	20	3.74	7.2	195
10	17.2	22	3.35	9.5	189
11	15.5	19	3.50	6	189
12	17.6	11	3.54	8.9	191
13	18.5	13	3.54	8.3	182
14	17.8	15	3.39	11.4	190
15	15.7	10	3.11	10.8	192
16	17.1	11	2.91	9.9	193
17	17.8	22	4.09	6.3	204
18	18.6	19	3.74	11.1	177
19	17.7	18	3.78	9.6	195
20	16.9	20	3.54	10.2	196
Average	16.8	19	3.5	8.5	193
Standard deviation	1.2	5	0.4	1.8	6

A.24. Table of tensile data for type I bundles twist 3 turns/inch.

Sample	Peak load (N)	Breaks at peak	Strain to failure (%)	Weibull modulus	Total breaks
1	17.3	16	4.21	4.9	204
2	18.1	13	3.50	5.8	197
3	18.5	15	3.35	6.6	155
4	18.4	25	3.58	5.7	182
5	17.0	11	3.43	5.6	190
6	17.9	8	3.31	7.7	186
7	19.7	12	3.35	6.9	174
8	16.6	17	3.70	6.7	158
9	17.0	7	3.90	6.9	172
Average	17.8	14	3.6	6.3	180
Standard deviation	1.0	5	0.3	0.9	17

A.25. Table of tensile data for type I bundles twisted 5 turns/inch.

Sample	Peak load (N)	Breaks at peak	Strain to failure (%)	Weibull modulus	Total breaks
1	16.7	20	3.15	5.9	198
2	16.4	22	2.91	6.8	172
3	17.7	31	2.91	3.9	174
4	19.1	35	2.99	6.2	185
5	13.2	34	3.23	6.0	201
6	19.1	16	2.99	8.3	164
7	17.9	24	3.23	4.1	133
8	17.0	13	3.23	7.8	191
9	15.1	40	2.91	6.0	204
10	16.1	21	3.27	5.9	178
11	18.8	16	2.83	5.7	138
Average	17.0	25	3.1	6.1	176
Standard deviation	1.8	9	0.2	1.3	24

List of References

Agarwal, B. D. and L. J. Broutman. 1995. Fibers, matrices, and fabrication of composites. Chapter 2 in *Analysis and Performance of Fiber Composites*. New York: John Wiley & Sons, Inc.

Cameron, N. M. 1968. The effect of environment and temperature on the strength of E-glass fibres. Part 2. Heating and aging. *Glass Technology*. **9** [5] : 121-130.

Coleman, B. D. 1958. On the strength of classical fibres and fibre bundles. *Journal of the Mechanics and Physics of Solids*. **7**: 60-70.

Cowking, A., A. Attou, A. M. Siddiqui, M. A. S. Sweet and R. Hill. 1991. Testing E-glass fibre bundles suing acoustic emission. *Journal of Material Science*. **26**: 1301-1310.

Dibenedetto, A. T. and P. J. Lex. 1989. Evaluation of surface treatments for glass fibers in composite materials. *Polymer Engineering and Science*. **29** [8] : 543-555.

Ema, K., H. Shigekawa and S. Hyodo. 1984. Acoustic location of fracture origin in optical glass fibers. *Communications of the American Ceramic Society*. **C**: 104-105.

Gücer, D. E. and J. Gurland. 1962. *Journal of the Mechanics and Physics of Solids*. **10**: 365-373.

Hill, R. and E. U. Okoroafor. 1995. Weibull statistics of fibre bundle failure using mechanical and acoustic emission testing: the influence of interfibre friction. *Composites*. **26** [10] : 699-705.

Hull, D. 1981. Fibers and matrices. Chapter 2. *An Introduction to Composite Materials*. Cambridge, U.K.: Cambridge University Press.

Jones, J. E., G. N. Haddad and J. E. Sutton. 1971. Tensile characteristics of twisted continuous-filament glass yarns. *Textile Research Journal*. **11**: 900-904.

Owens–Corning Corp. 1983. Product literature. *Owens-Corning Technical Report*, March 1983.

Phoenix, S. L. 1974. Probabilistic strength analysis of fibre bundle structures. *Fibre Science and Technology*. **7**: 15-31.

Plueddemann, E. P. 1991. Silane coupling agent adhesion. Chapter 9. *Fundamentals of Adhesion*. ed. Lieng-Huang Lee. New York, NY: Plenum Publishing Corporation.

Thomas, W. F. 1971. An investigation of the factors affecting the strength of glass fibre strand. *Glass Technology.* **12** [3] : 60-64.

Thomas, W. F. 1972a. An investigation of the factors affecting the strength of glass fibre strand. Part 2. *Glass Technology*. **13** [1] : 17-21

Thomas, W. F. 1972b. An investigation of the factors affecting the strength of glass fibre strand. Part 3. The strength in polyester resin. *Glass Technology*. **13** [4] : 122-125

Thomas, W. F. 1972c. An investigation of the factors affecting the strength of glass fibre strand. Part 4. The effect of fibre surface area. *Glass Technology*. **13** [5] : 141-144

Weibull, W. 1951. A statistical distribution function of wide applicability. *Journal of Applied Mechanics*. **18** [9] : 293-297

Whitney, J. M. 1966. Geometrical effects of filament twist on the modulus and strength of graphite fiber-reinforced composites. *Textile Research Journal*. **36** [9] : 765-770

Zweben, C., W. S. Smith and M. W. Wardle. 1979. Test methods for fiber tensile strength, composite flexural modulus, and properties of fabric-reinforced laminates. *Composite Materials: Testing and Design.* Fifth Conference. ASTM STP 674

Vita

Amanda Kay Davis was born in Alton, Ill., on August 28, 1975. She graduated as valedictorian from Civic Memorial High School in Bethalto, Ill. She then attended the University of Illinois at Urbana–Champaign and earned a Bachelor of Science in Engineering Mechanics in May 1997. In August 1997, she entered the master' s program in the Theoretical and Applied Mechanics Department at the University of Illinois at Urbana–Champaign, where she was a teaching assistant for a semester and a research assistant under the guidance of Professor Nancy R. Sottos. She was hired by AlliedSignal' s Engine Division in Phoenix, Ariz., in August 1999.